USING CONCURRENT TRANSMISSIONS TO IMPROVE THE RELIABILITY AND LATENCY OF LOW-POWER WIRELESS MESH NETWORKS

Von der Fakultät für Elektrotechnik und Informationstechnik der Rheinisch-Westfälischen Technischen Hochschule Aachen zur Erlangung des akademischen Grades eines

Doktors der Ingenieurwissenschaften (Dr.-Ing.)

genehmigte Dissertation vorgelegt von

Antonio David Escobar Molero, MSc.
aus Almería, Spanien

Berichter: Universitätsprofessor Dr.-Ing. Stefan Heinen

Universitätsprofessor Dr. Petri Mähönen

Tag der mündlichen Prüfung: 18.03.2020

Diese Dissertation ist auf den Internetseiten der Universitätsbibliothek online verfügbar.

USING CONCURRENT TRANSMISSIONS TO IMPROVE THE RELIABILITY AND LATENCY OF LOW-POWER WIRELESS MESH NETWORKS

Doctoral Thesis

ANTONIO DAVID ESCOBAR MOLERO

ABSTRACT

Concurrent Transmissions (CT) occur when different transmitters simultaneously send *the same* packet. We analyze how CT distort the received waveform and characterize the Bit Error Rate (BER) of a receiver trying to recover the original bitstream. If collisions are not completely destructive and the information can still be recovered, then simple, robust and latency-optimal wireless mesh protocols can be designed. These protocols are particularly suitable for low-cost and low-power Internet of Things (IoT) applications, especially in high-interference scenarios, where routing efforts can be cumbersome and flooding becomes more effective.

Distortion introduced by CT has two main causes. Firstly, simultaneous transmitters are not perfectly synchronized, which introduces intersymbol interference (ISI). The ISI can be reduced by keeping the synchronization mismatch below half the symbol period. Secondly, there is a periodical energy fading (beating) in the received waveform due to alternating patterns of constructive and destructive interference. This beating cannot be avoided, since it is originated by the non-coherent nature of the different local oscillators in the transmitters. Only communication systems able to cope with periodical amplitude and phase distortions are suitable for CT-based protocols.

Communication performance is analyzed for typical phase- and frequency-modulation systems, obtaining the first closed-form analytical expression for the BER of two non-coherently received Frequency-Shift Keying (FSK) transmissions. For more complex systems, simulated BER curves are obtained. We conclude that CT are extremely destructive in conjunction with amplitude and phase modulations, but work particularly well with FSK modulations.

In non-coherent FSK systems, the efficiency of CT depends on the level of external noise, being very effective in dense and high-noise environments. Demodulators based on non-coherent FSK receivers are typically used in two popular low-power IoT proto-

cols: Bluetooth 5 and IEEE 802.15.4. Both are perfect candidates for CT-based mesh protocols.

Finally, two CT-based award-winning protocols are designed: RedFixHop and BigBangBus. RedFixHop is the first protocol using the concept of disseminating information with concurrent packet acknowledgments (ACKs), while BigBangBus proposes the novel usage of longer preambles to decrease the BER introduced by the CT. Both protocols haven been tested in multiple competitions, repeatedly beating state-of-the-art solutions in terms of energy efficiency, reliability and end-to-end latency.

CONTENTS

LIST OF FIGURES

LIST OF TABLES

ACRONYMS

ACK Acknowledgment

AI Artificial Intelligence

ASK Amplitude-Shift Keying

AWGN Additive White Gaussian Noise

BER Bit Error Rate

BFSK Binary Frequency-Shift Keying

BLE Bluetooth Low Energy

Bluetooth SIG Bluetooth Special Interest Group

BPSK Binary Phase-Shift Keying

CDF Cumulative Distribution Function

CI Constructive Interference

CPFSK Continuous-Phase Frequency-Shift Keying

CRC Cyclic Redundancy Check

CSMA Carrier-Sense Multiple Access

CT Concurrent Transmissions

DCO Digitally Controlled Oscillator

DPSK Differential Phase-Shift Keying

DSSS Direct Sequence Spread Spectrum

DVB Digital Video Broadcasting

EWSN International Conference on Embedded Wireless Systems and Networks

FPGA Field-Programmable Gate Array

FSK Frequency-Shift Keying

GFSK Gaussian Frequency-Shift Keying

IoT Internet of Things

ISI Intersymbol Interference

LQI Link Quality Indicator

LPWAN Low-Power Wide-Area Network

MSK Minimum-Shit Keying

OFDM Orthogonal Frequency-Division Multiplexing

OOK On-Off Keying

OQPSK Offset Quadrature Phase-Shift Keying

PDF Probability Density Function

ppm parts per million

BPSK Binary Phase-Shift Keying

QAM Quadrature Amplitude Modulation

QPSK Quadrature Phase-Shift Keying

RSSI Received Signal Strength Indicator

SDR Software-Defined Radio

SFD Start Frame Delimiter

SFN Single-Frequency Network

SIR Signal-to-Interference Ratio

ST Synchronous Transmissions

TDMA Time-Division Multiple Access

UWB Ultra-Wide Band

VANET Vehicular ad-hoc Network

WSAN Wireless Sensor and Actuator Network

WSN Wireless Sensor Network

Part I

INTRODUCTION

1 INTRODUCTION

Protocols based on Concurrent Transmissions (CT) exploit the following effect:

different transmitters sending the same bitstream, when tightly synchronized, interfere non-destructively with a certain probability, which means that packet reception is feasible, even when multiple transmissions simultaneously coexist in the air.

In contrast, when concurrent transmitters send packets with different payloads, or their synchronization is not tight enough, packets normally collide (*interfere destructively*), rendering reception impossible. CT are usually misunderstood, since the effect is mainly analyzed in the baseband domain, neglecting wave superposition effects. Because of wave interference properties, CT-based protocols do not work with every modulation scheme, in particular they are not suitable for complex constellations and high-bandwidth technologies, like WiFi [28]; but they are very effective and efficient for simple frequency modulations [24], like non-coherently received IEEE 802.15.4 and Bluetooth Low Energy (BLE).

A comprehensive analysis including the effects of the carrier, able to predict the technologies that work with CT, is missing in the literature, currently being mostly a matter of trial and error. The exploitation of CT in WSNs has already been experimentally demonstrated in protocols like Glossy [26], but a rigorous theoretical explanation of the effect is missing. The objective of this thesis is filling this gap, increasing the awareness and knowledge of CT, addressing their real working principles, in both analytical and experimental levels. Furthermore, we want to demonstrate that CT-based flooding protocols are a powerful tool to develop simple and reliable latency-optimal wireless mesh protocols, able to beat state-of-the-art alternatives in low-power and low-bandwidth WSNs.

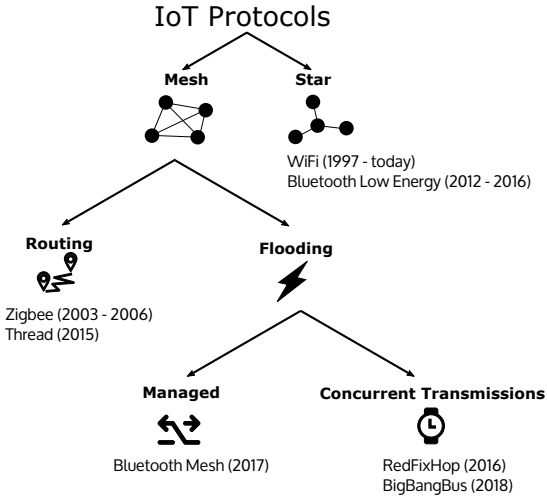

Figure 1.1: Classification of some IoT protocols, including those introduced in the thesis (RedFixHop and BigBangBus)

1.1 MOTIVATION AND OBJECTIVES

Cellular Internet of Things (IoT) enables breakthrough applications with technologies like Sigfox, LoRa, NB-IoT, LTE-M and ultimately, 5G. Affordable and low-power connected devices can directly communicate with internet from virtually every location with mobile coverage. Nevertheless, low-power cellular IoT is limited by coverage, capacity restrictions and costs imposed by network operators. Most applications integrating cellular connectivity only send a few messages per day [58]. On the other hand, the upcoming ultra-low latency modes of 5G are power-hungry, and the widely-defined goal of obtaining a bounded end-to-end latency smaller than 1 millisecond is extremely challenging, and will require costly base station deployments in critical factory environments [59].

However, new Artificial Intelligence (AI) applications require big-data for tasks like performance analytics, supply chain and predictive maintenance, which is not totally compatible with the cloud computing approach of cellular IoT. This has opened the

pathway for the appearance of new paradigms, such as *edge computing*, which benefit from the smaller latency and scalability improvements when data is processed closer to the end devices [7].

Mesh networks are the optimal choice for this type of application. In a local mesh network, key parameters such as latency, scalability and bandwidth, can be fine-tuned to accurately match the application requirements. With mesh networks, we only need an Internet subscription for one device: the border-router or gateway. Every command is efficiently broadcast directly between edge nodes, with optimal latency and channel usage. The Internet link is only used for remote monitoring, actuation or security and commissioning tasks, removing a potential bottleneck. Only when the external computing and storage resources of the cloud are actually needed, costly and potentially high-latency communication links are used. Otherwise, local mesh links are enough, enabling a smoother user experience for tasks like lighting control. With multiple hops and paths, high-reliability and coverage are assured. Applications like home and building automation, retail beacons, smart metering, and industrial sensor and actuator networks, particularly indoors and in hard to reach areas, like basements, greatly benefit from mesh topologies.

The most widely used IoT protocols for mesh networks are Zigbee and Thread. Zigbee, established in 2003, is the most mature, and has been successfully used for many Wireless Sensor Network (WSN) applications in smart cities. Thread, tailored to the smart home market and established in 2015, benefits from the recent advances in Internet protocols, featuring native IP-based connectivity (6LoWPAN), providing seamless interoperability with cloud-based resources.

Thread and Zigbee are routing-based. During our research, the new Bluetooth Mesh standard was published. It came to light in 2017 and uses flooding instead of routing. It is the first mainstream protocol that showcases flooding as a serious alternative to routing in standard mesh networks. To justify the usage of flooding in their flagship protocol, the Bluetooth Special Interest Group (Bluetooth SIG) uses a similar reasoning to the one we came up with; validating our prediction regarding the upcoming trend of flooding-based mesh networks. With flooding, the communica-

tion is inherently multipath, avoiding single points of failure and preventing network interruptions in the presence of interference or node malfunctions.

Our novel approach to flooding is different from the one used by Bluetooth Mesh. They propose a randomly-scheduled flooding (*managed flooding*), which can experience reliability and scalability issues [5]. In contrast, we use a more advanced and smart flooding mechanism, based on CT, that relies on tightly synchronizing all the retransmissions to minimize the chance of collision. It optimizes the packet reception rate, even in the noisiest environments, thanks to featuring outstanding spatial, frequency and temporal diversities.

We want to demonstrate that, exploiting CT-based flooding, extremely simple and robust wireless mesh networks can be deployed, beating state-of-the-art solutions in terms of reliability and latency. To fulfill the goal and validate our assumption, we decided to attend the event in which the highest number of publications regarding CT have been published in the last years, the International Conference on Embedded Wireless Systems and Networks (EWSN). There, we competed in the Dependability Competition, beating all competing routing- and flooding-based solutions in the 2016, 2017 and 2019 editions, using our novel CT-based flooding protocols (RedFixHop [36], BigBangBus [23] and RedNodeBus [25]). In addition to the experimental evidence, in the thesis we develop a solid analytical and simulation framework, going beyond the existing literature, in order to increase the awareness and rigorous knowledge of CT.

1.2 THESIS STRUCTURE

The thesis is structured in five different parts:

A. Part i, containing Chapters 1 and 2, is the introduction of the thesis. In Chapter 1, we set the goals and introduce CT and their applicability to mesh IoT networks as the main motivation for the work. In Chapter 2, we present a comprehensive state-of-the-art analysis of current advances in CT.

B. Part ii comprises Chapters 3, 4 and 5. It includes analytical and simulation models of the CT. In Chapter 3, we lay the foundation for the analysis of the CT effect, starting with the baseband model and addressing the importance of maintaining a tight synchronization between the concurrent transmitting nodes. In Chapter 4, the important distortion (beating) introduced by the carrier is presented. Finally, in Chapter 5, we demonstrate the applicability CT-based techniques in non-coherent Frequency-Shift Keying (FSK) communication systems, as those used in low-power IoT devices, by introducing the concept of *capture area*.

C. Part iii encompasses Chapters 6 and 7. There, we design and showcase protocols that make practical use of CT using commodity low-cost hardware, featuring optimal latency and reliability properties, with extremely efficient and effective results in real testbeds and competition environments. RedFixHop protocol is introduced in Chapter 6, while BigBangBus is presented in Chapter 7.

D. Part iv only includes Chapter 8, in which the obtained results are summarized and suggestions for future research lines are discussed.

E. Part v includes Appendix A, in which mathematical details of the models used for the simulations are added. We believe that this is the first work that shows an analytical expression for the Bit Error Rate (BER) in the presence of CT that matches simulated and experimental results (Eq. A.29).

2

STATE OF THE ART

Traditionally, most successful wireless protocols are those based on simple architectures, mainly point-to-point links (e.g. Bluetooth Classic) or star topologies (Wi-Fi). Mesh networks, involving multiple hops, are thought to be complex to design and analyze, due to the dynamic routing efforts that are required. Similarly, typical mechanisms to access the medium and start a transmission are basically asynchronous and using simple decisions based on energy detection mechanisms, like Carrier-Sense Multiple Access (CSMA).

This is enough when the wireless channel is not crowded and devices do not have tight energy constraints. Complex multi-hop mesh WSNs were used mainly in the academic field or in very specialized large-scale deployments, in applications like smart cities and environmental monitoring, based on mature technologies like Zigbee [1]. Even when long-range communications are required, IoT connectivity is normally solved using legacy cellular technologies (2G/GSM/GPRS), operating in the corresponding licensed frequency bands or, more recently, star topology-based Low-Power Wide-Area Network (LPWAN) technologies like LoRa and Sigfox, operating in unlicensed bands [10].

Nowadays, with the introduction of billion of IoT devices in the wireless ecosystem [9], communication protocols have new requirements. With novel paradigms, like edge computing, data processing in the end nodes increases, in order to address the concerns of response time, battery life, bandwidth, cost savings, as well as data safety and privacy [50]. Unicast communication between nodes, through a cloud, and asynchronous transmissions are neither efficient nor scalable enough to accommodate novel low-power and low-latency applications in many fields, like lighting or real-time industrial scenarios. Therefore, research in the area of mesh networks and synchronized transmissions has experienced a renewed interest.

In particular, for resource-limited networks, where memory and power consumption constraints apply, flooding protocols constitute and appealing mechanism to deploy multi-hop mesh networks, as Bluetooth Mesh showcases. During the thesis, we will focus on the theoretical, simulated and experimental analysis of a promising novel subset of flooding protocols, those based on CT.

2.1 FROM CONSTRUCTIVE INTERFERENCE TO CONCURRENT TRANSMISSIONS

Glossy [26], published in 2011, is one of the first protocols that popularized the usage of the so-called Constructive Interference (CI) as a mechanism to achieve multi-hop network flooding and time synchronization. Multiple publications followed, generally considering CI as the effect that allows a receiver to decode a packet that is simultaneously sent by multiple transmitters. By contrast, if the packet cannot be recovered, interference is considered to be destructive [4]. To achieve CI-based flooding, simultaneous transmissions must be tightly synchronized. As a mantra, the maximum temporal displacement for CI to be triggered is considered to be 0.5 μs in IEEE 802.15.4 [26], derived from experimental results and baseband interference considerations on the bit waveforms [44].

Since 2016, the term CI has been progressively abandoned, since it could lead to misinterpretations of the actual wave interference pattern [38]. No purely constructive interference is ever observed, but an alternating temporal pattern of constructive and destructive periods [24]. Simultaneous transmissions do not generally lead to any performance gain, as the term *constructive* may suggest. On the contrary, CI-based flooding has scalability issues, since the transmission progressively degrades as the number of simultaneous transmitter increases [44]. Nowadays, the terms CT or Synchronous Transmissions (ST) are preferred to CI [57][61][33]. It stresses the fact that, although reception is feasible as long as a tight synchronization among the transmitters is maintained, the quality of the transmission actually decreases. CT performance has been widely analyzed, including the impact of the differences

in the hardware of the transceivers [63], and the possibilities using Software-Defined Radio (SDR) [64].

2.2 EFFECTS RELATED TO CONCURRENT TRANSMISSIONS

CT analysis has similarities with the classic *capture effect* observed in frequency modulations [27], with the main difference that in CT all the simultaneous transmitters are synchronized and sending exactly the same bitstream. The term capture effect usually refers to the ability of the receiver to decode a packet in the presence of multiple and unsynchronized transmissions of *different* payloads. The capture effect is normally triggered when the receiver locks with the most energetic transmission, as is the case when the most energetic packet arrives to the receiver before it has started receiving a weaker one [27].

CT are also related to classic multipath analysis and fading effects, but in CT the simultaneously received waveforms are non-coherent, while in multipath they all come from the same transmitter and constant phase relationships can be considered. This non-coherent property is what gives CT their characteristic periodical amplitude beating [24].

Similarly, CT-based protocols share characteristics with the concept of Single-Frequency Network (SFN) used in in terrestrial Digital Video Broadcasting (DVB) [45]. With SFNs, a efficient use of the spectrum is achieved by simultaneously broadcasting the same signal over the same frequency channel in adjacent transmitting cells. The main difference between CT-based mesh networks and SFNs is that an external source, typically GPS, is used as a common reference for time and frequency synchronization between the broadcasters. On the other hand, in mesh networks using CT, packet receptions from the previous hop of the network are used for time synchronization (and data dissemination), and no external common temporal reference is typically available. Furthermore, SFNs are commonly used in high data rate systems, for example to transmit high-definition multimedia signals in DVB. In SFNs, distortion is attenuated using complex equalization and modulation techniques, such as Orthogonal Frequency-Division Multiplexing (OFDM) with guard intervals, interleaving

and error-correcting codes, normally impractical for low-power and low data rate IoT transceivers.

2.3 FLOODING PROTOCOLS BASED ON CONCURRENT TRANSMISSIONS

Flooding networks are simple, reliable and scalable. No complex routing table creation and management are required, since the communication is inherently multipath, avoiding single points of failure and preventing network interruptions in the presence of interference or node failures. Flooding constitutes the perfect choice for scenarios in which the communication is essentially multicast, like in lighting applications, where a single switch can control hundreds of lights. They are also not necessarily power inefficient, if proper network scheduling mechanisms are used [23].

Since Glossy, most flooding protocols based on CT have been designed for low-power IoT networks, in particular to operate with the IEEE 802.15.4 physical layer [26][11][3][60]. They proved very successful in the Dependability Competition of the EWSN, winning all of the four first editions (2016 [36], 2017 [40], 2018 [23] and 2019 [25]). In the competition, CT-based mesh networks proved superior to classic routing schemes transmitting short packets in harsh environments, in terms of reliability, latency and power consumption. Simplicity is also an advantage, since no route discovery and maintenance are needed; what can be cumbersome in scenarios with high levels of noise and frequency-hopping jamming [19].

Due to the success of CT-based synchronous flooding, its applicability has been tested in other physical layers, like BLE [2], LoRa [39] and Ultra-Wide Band (UWB) [35] [13]. Furthermore, flexible stacks and communication frameworks including the CT-based communication primitive are appearing [33].

Security is also a concern; CT-based networks are prone to packet injection attacks [29][30][31], since the tight synchronization required when scheduling the retransmissions makes it challenging to authenticate the packets before repeating them.

2.4 APPLICATIONS OF LATENCY-OPTIMAL CT-BASED PROTOCOLS

There is a growing trend towards simple star networks and cloud-based topologies, removing the routing complexity from the end devices, as the cellular IoT becomes a reality with technologies like NB-IoT, LTE-M, and, ultimately, with the 5G technological ecosystem. They enable cheap and low-power devices to directly communicate with internet resources using the cellular network, without additional gateways [49]. In the meantime, LPWAN technologies like LoRa and Sigfox provide solutions for outdoor connectivity in those scenarios where low latency and high bandwidth are not required, and communication is asymmetrical and infrequent, mainly from the sensor nodes to the cloud. Furthermore, in indoor scenarios, the upcoming Wi-Fi standard, 802.11ax, starts the transition from a 'best-effort' approach to a more deterministic behavior, with synchronous mechanisms to accommodate a multitude of devices with different needs, from low-resource and battery-operated use cases to complex and high-bandwidth multimedia applications [6].

Nevertheless, mesh networks are the optimal choice for applications like lighting, home and building automation, retail beacons, smart metering, and industrial sensor and actuator networks. They allow to further reduce power consumption, extend the communication range and improve the overall system reliability. Furthermore, direct end-to-end communication can dramatically improve the user experience, since the response latency can be greatly decreased. This is particularly critical for real-time networks or closed-loop control in WSANs [41][42].

The most widely used IoT protocols for mesh networks are Zigbee and Thread, both based on IEEE 802.15.4 and routing. Zigbee, established in 2003, is the most mature. Thread, tailored to the smart home market and established in 2015, benefits from the recent advances in the Internet protocols, featuring native IP-based connectivity, providing a seamless connectivity with internet cloud-based resources. Bluetooth Mesh, established in 2017, is the most recent addition, featuring direct smartphone connectivity and managed flooding instead of routing.

Bluetooth Mesh is the first example that showcases flooding as a serious alternative to routing in standard mesh networks. Nevertheless, the proposed randomly-scheduled flooding (*managed flooding*) experiences scalability issues [5], which can be circumvent with novel CT-based synchronous flooding. Furthermore, CT-based flooding is a great fit for novel applications, like RF energy harvesting [14][51] and VANETs [34][65].

Part II

THEORETICAL ANALYSIS AND SIMULATIONS

A comprehensive analysis on the Concurrent Transmissions (CT) effect in WSN, some time misleadingly called Constructive Interference, is missing in the literature. In the following chapters, an accurate description of the real causes and consequences derived from the interference of CT is performed. Starting with the straightforward baseband analysis, scalibility figures and BER are calculated for typical digital phase- and frequency-modulation systems. One important analytical tool, the capture area, is introduced to differentiate the systems where CT-based protocols can be effectively used.

3

BASEBAND ANALYSIS OF CONCURRENT TRANSMISSIONS

In order to understand the effects of CT on the wireless link performance, we start by considering the impact on the baseband domain, removing the effects of frequency and phase differences in the carriers of the simultaneously transmitted signals.

The main error source is the existing temporal displacement between transmissions from different sources, due to unavoidable timing errors. Temporal errors can be caused by software delays, due to the application running on the main microcontroller or variable jitter in the radio transceiver while processing the retransmissions. Different operating conditions (temperature, supply voltage, etc.) and manufacturing tolerances make it impossible to avoid small errors.

Using the communication model of Fig. 3.1, we analyze the maximum tolerable time displacement between two CT before bit errors appear in the following situations:

A. Ideal case with square waveforms and no noise (Section 3.1).

B. Using raised-cosine pulse shaping and no noise (Section 3.2)

C. In Additive White Gaussian Noise (AWGN) channels (Section 3.3).

Then, we extend the discussion to scenarios with more than two concurrent transmitters (Section 3.4).

3.1 THE IDEAL CASE: TWO TRANSMITTERS AND RECTANGULAR WAVEFORMS

Assuming an ideal rectangular pulse and an infinite bandwidth channel, we start our analysis with the interference of antipodal

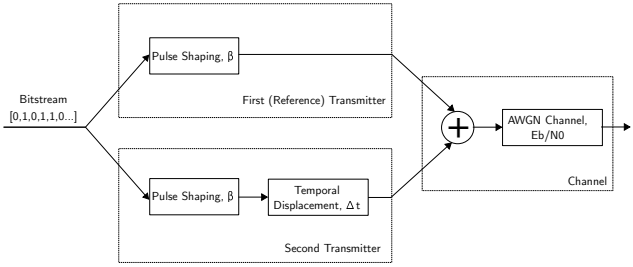

Figure 3.1: Proposed communication system for the baseband analysis of two concurrent transmitters

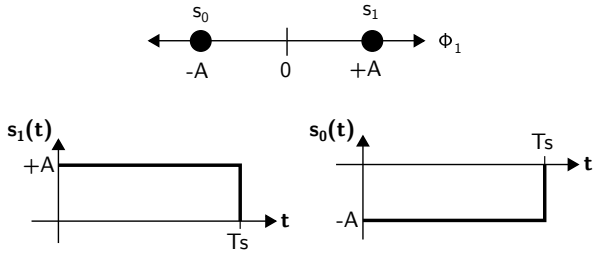

Figure 3.2: Ideal rectangular antipodal waveforms

rectangular waveforms (Fig. 3.2), which model the baseband behavior of modulations like coherently-detected BPSK; but similar results can be obtained for other systems. In particular, the BER in AWGN channels for Quadrature Phase-Shift Keying (QPSK), Offset Quadrature Phase-Shift Keying (OQPSK) and coherently-detected Minimum-Shit Keying (MSK) are ideally the same as in BPSK, since the main difference is the addition of an equivalent orthogonal transmission channel to the constellation.

We suppose two transmitters sending the same bitstream with a relative temporal displacement, Δt, and a symbol period, T_S. Both symbols are equally probable and signals from both transmitters are received with the same power level. This is a worst-case scenario, since most receivers are able to improve their performance by synchronizing with the strongest signal, assuming small temporal displacements ($\Delta t < T_S$). Similar power levels between the interfering signals generally impose the hardest con-

ditions to the receiver, since there is no dominant, stronger signal to exploit advantages like the capture effect (Section 2.2). The receiver is perfectly synchronized with one of the transmitters, which is the reference from which Δt is defined. Since, at the moment, we want to characterize only the error due to the temporal misalignment, no noise is considered. The receiver is an optimum AWGN receiver based on the maximum-likelihood criterion [48].

In this scenario, we can derive an expression for the BER analyzing three different cases:

A. When the time displacement, Δt, is smaller than the symbol period, T_S, and no noise is considered, no errors are introduced. Since both transmitters are sending the same bitstream, the correct bit is always correlated with higher energy in the receiver.

B. When Δt is a whole multiple of T_S, considering a random bitstream, 50% of the times a collision between two different bits happens. In this situation, the output of the receiver is undefined. Since both bits are correlated with the same (zero) energy, the decision is random. With 50% probability the output of the receiver will be the right one. Combining both probabilities we get a 25% error rate in this case.

C. Otherwise, there are only errors if the interfering transmitter is sending two consecutive bits of opposite sign, what happens with 25% probability. In this situation, the output of the receiver is again undefined, demodulating the right bit with 50% probability. Combining both effects, we get a 12.5% error rate.

As a result, the following piecewise-defined function for the BER is obtained (Fig. 3.3):

$$BER_{ideal\,2\,Transmitters}(\Delta t) = \begin{cases} 0 & if\ \ |\Delta t| < T_S \\ 0.25 & if\ \ |\Delta t| = nT_S\ for\ n = 1, 2, 3... \\ 0.125 & otherwise \end{cases} \tag{3.1}$$

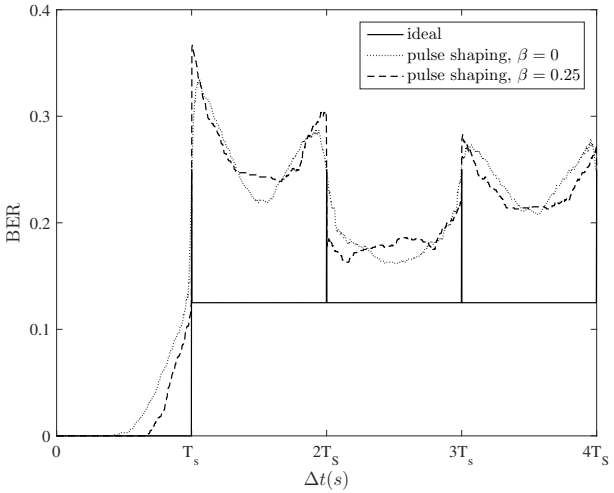

Figure 3.3: BER for different time displacements in the ideal case (rectangular pulses) and with pulse shaping (no noise)

Our first important result is:

in the ideal baseband model, the temporal displacement, Δt, between CT must be, at least, smaller than the symbol period, T_S.

As we will discuss in the following sections, in a realistic analysis including noise, BER discontinuities are removed, and smooth curves are obtained. An accurate threshold for the temporal displacement with pulse shaping and noise is lower. Nevertheless, the analytical expression for the ideal case is useful as a first approximation to understand the effect and the periodic peaks of the BER; since a characteristic effect of CT is that, when the time displacement, Δt, is a multiple of the symbol period, T_S, a peak in the BER appears, degrading the communication performance.

3.2 TWO CONCURRENT TRANSMITTERS IN BANDWIDTH LIMITED CHANNELS

The previous result assumed an ideal situation with rectangular signals. In a practical scenario, with the presence of AWGN noise

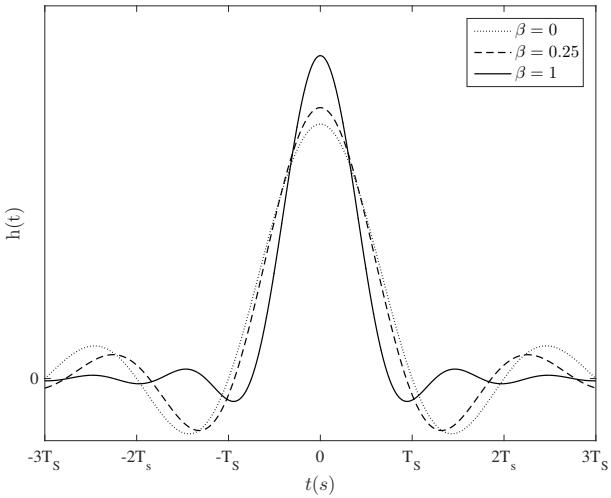

Figure 3.4: Impulse response of a square-root-raised-cosine filter for different roll-off factors normalized to unit energy

and bandwidth-limited channels, pulse shaping is employed to reduce the bandwidth of the transmitted symbols.

In order to get more accurate results, we simulate the system running a stochastic (Monte Carlo) simulation in MATLAB. We add to the communication system, in the transmitting and receiving sides, a typical pair of square-root-raised-cosine matched digital filters with different roll-off factors, β, (Fig. 3.4) truncated with a rectangular window of 32 symbols (16 symbols delay in the demodulation). We still consider that signals from both transmitters are received (added) with the same power.

Now, we get a continuous curve for the BER (Fig. 3.3), which more accurately represents the results obtained in experimental scenarios. As the roll-off factor, β, decreases, the BER starts increasing with lower temporal displacements, Δt, since we have higher energy in the time-domain side lobes (Fig. 3.4) and the misalignment is more harmful. As a result, we derive a more conservative statement:

due to pulse shaping effects, the temporal displacement, Δt, between CT must be smaller than half the symbol period, $T_S/2$.

3.3 TWO CONCURRENT TRANSMITTERS IN AWGN CHANNELS

We still lack an accurate comprehensive explanation of the effect of CT when the temporal displacement is less than half the symbol period. To solve this and complete our baseband analysis with two transmitters, we repeat the Monte Carlo MATLAB simulation adding different levels of AWGN to the received symbols, for a fixed roll-off factor, $\beta = 0.25$.

We define the energy per bit to noise power spectral density ratio (E_b/N_o), as the ratio between the energy of one of the transmissions and the noise. We consider both transmissions as having the same energy, and thus their received waveforms have the same amplitude ($A_1 = A_2$). Assuming A_1 referenced to a unit resistor, E_b/N_ocan be defined as:

$$\frac{E_{b\ Baseband}}{N_0} = \frac{(A_1)^2}{N_0} T_S \tag{3.2}$$

We obtain the results of Fig. 3.5 and Fig. 3.6. For only one transmitter, the results are the expected for an antipodal constellation (Fig. 3.2):

$$BER_{1\ Transmitter} = Q\left(\sqrt{\frac{2E_b}{N_0}}\right) \tag{3.3}$$

In addition, we further validate the previous affirmation of establishing half the symbol period, $T_S/2$, as a conservative value for the maximum allowed temporal displacement. Above $T_S/2$, the performance degrades quickly, rapidly achieving worse results than those observed with only one transmitter.

Since we define E_b/N_0 relative to the energy of only one transmitter, with small temporal displacements and several transmitters, a performance gain is observed:

when the temporal displacement, Δt, is lower than half the symbol period $T_S/2$, constructive baseband interference and improved resistance against AWGN is observed, obtaining a smaller BER with two synchronized concurrent transmitters than with only one transmitter, at the

cost of doubling the power requirements (transmission from two different sources).

The maximum gain in E_b/N_0 is 6 dB, when both transmissions are perfectly synchronized *($\Delta t = 0$);* since this is equivalent to sending with only one transmitter with double the amplitude of the field (and four times the energy):

$$\frac{(A_1 + A_2)^2}{N_0} T_S = 4\frac{(A_1)^2}{N_0} T_S = 4E_{b\ Baseband} \tag{3.4}$$

This might seem counterintuitive, but it is only an artifact introduced by the baseband analysis. Analyzing superposition and interference of real waves, an alternating pattern of constructive and destructive interference is seen at the receiver-side, following the principles of energy conservation [16], and never experiencing and average energy gain bigger than 3 dB, as expected.

In the following chapters, we will analyze practical carrier-based systems. Pure constructive interference is not physically possible with systems working at high frequency, involving modulating a carrier and the spatial propagation of spherical waves generated by independent oscillators (non-coherent sources), with frequency and phase differences, and separated by a distance much higher than the wavelength.

Practically, the second transmitter, *even if tightly synchronized*, generally appears as a harmful interference that decreases the performance. This is particularly true for uncoded transmissions and hard-decision receivers in coherently-detected amplitude- and phase-modulated systems. As we will see in the following chapters, the gain experienced by using CT-based protocols is exploited in very noisy environments and dense mesh networks, where the superposition of a multitude of transmissions can beat the noise and greatly simplify the routing effort.

3.4 MULTIPLE TRANSMITTERS IN BASEBAND: SCALABILITY ISSUES

Temporal displacements between CT follow a normal distribution, as it is affected by a different number of independent processes.

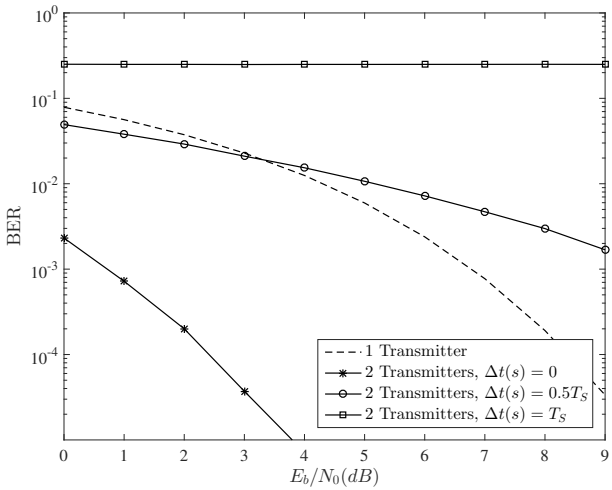

Figure 3.5: BER for two concurrent transmitters with different noise levels and time displacements (baseband, I)

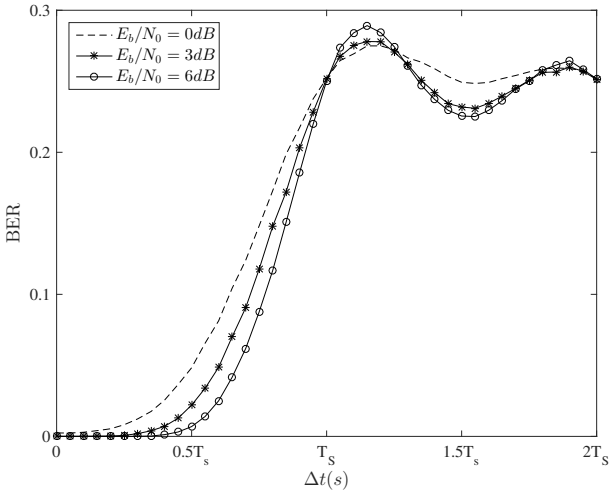

Figure 3.6: BER for two concurrent transmitters with different noise levels and time displacements (baseband, II)

They can be treated as independent, normally distributed random variables, each with the same variance, σ^2, considering that all the transmitters have similar hardware and software delays. This variance may appear because of non-deterministic processing times in the microcontroller and radio transceiver, or due to limitations imposed by their clock frequencies. It can be properly characterized through experimental measurements with the real hardware and software set-up.

We can model the equivalent temporal displacement, Δt_{eq}, between N concurrent transmitters as a random variable, ΔT_{eq}, following a normal distribution with its equivalent variance being the sum of the variances, $N\sigma^2$, and zero average. We define the Probability Density Function (PDF) (for $N \geqslant 2$):

$$PDF_{\Delta T_{eq}}(\Delta t_{eq}, N, \sigma^2) = \frac{1}{\sqrt{2\pi N\sigma^2}} \exp\left(-\frac{{\Delta t_{eq}}^2}{2N\sigma^2}\right) \tag{3.5}$$

And the Cumulative Distribution Function (CDF) of the equivalent temporal displacement for N transmitters is defined as (for $N \geqslant 2$):

$$CDF_{\Delta T_{eq}}(\Delta t_{eq}, N, \sigma^2) = \frac{1}{2}\left[1 + erf\left(\frac{\Delta t_{eq}}{\sqrt{2N\sigma^2}}\right)\right] \tag{3.6}$$

In Fig. 3.7 and Fig. 3.8 we observe the PDF and CDF of the equivalent temporal displacement. It can be seen how increasing the number of concurrent transmitters, the probability of a higher equivalent temporal displacement is also increased, potentially degrading the performance of the communication.

Assuming that all the CT are received with the same power level, we can introduce this expression in the BER equation for the ideal case with two transmitters (Eq. 3.1). We extend it to describe the BER for N transmitters, each with equal temporal variance, σ^2 (for $N \geqslant 2$):

$$BER_{ideal\ N\ Transmitters}(N, \sigma^2) = 0.125\left[1 - erf\left(\frac{T_S}{\sqrt{2N\sigma^2}}\right)\right] \tag{3.7}$$

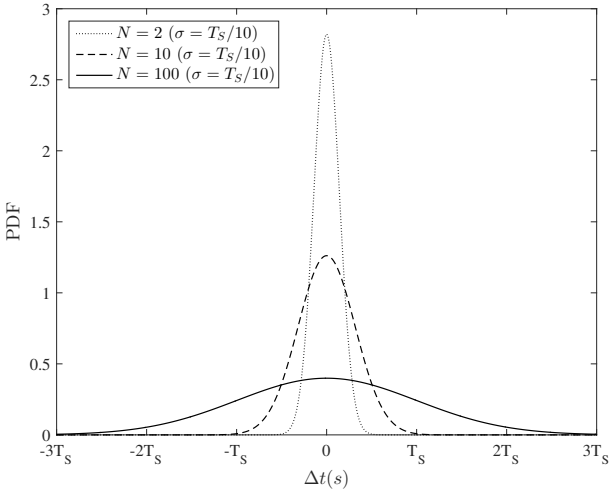

Figure 3.7: PDF of the equivalent temporal displacement for multiple transmitters

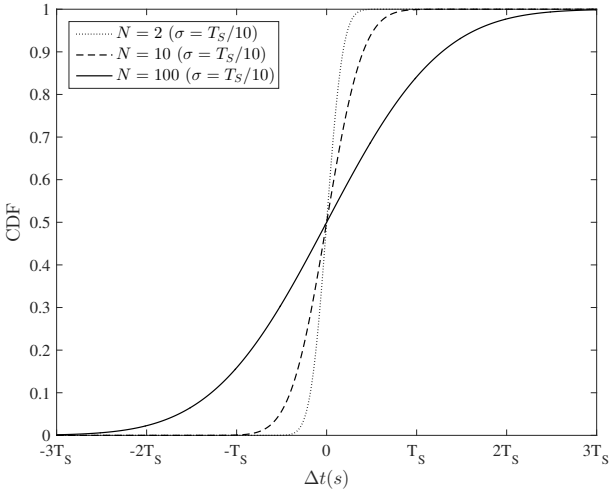

Figure 3.8: CDF of the equivalent temporal displacement for multiple transmitters

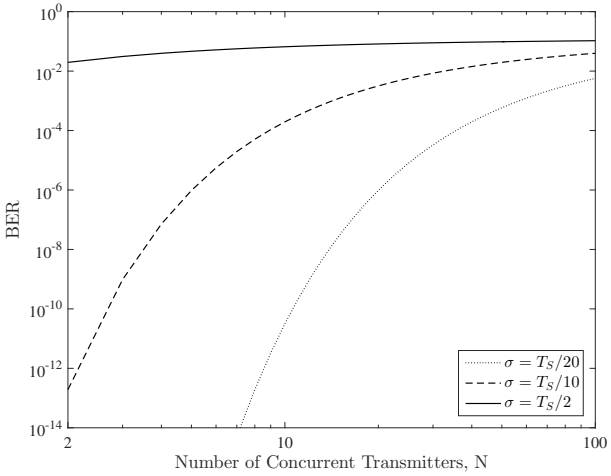

Figure 3.9: BER for multiple transmitters in the ideal case (rectangular pulses and no noise)

As seen in Fig. 3.9, with the ideal baseband model, the performance rapidly degrades when increasing the number of concurrent transmitters, tending to a successful bit reception ratio of 87.5%.

Following the 68-95-99.7 rule for normal distributions, we can impose half the symbol period, $T_S/2$, to be within three standards deviations, assuring that only 0.3% of the transmissions have an equivalent temporal displacement, Δt_{eq}, higher than $T_S/2$, what we established as a realistic threshold in previous sections. We get the following threshold for the maximum number of concurrent transmitters:

$$N < \left(\frac{T_S}{6\sigma}\right)^2 \tag{3.8}$$

This is an important result for network planning and design, since it shows that, to accommodate a bigger number of CT, we need to either reduce the bit rate by increasing the symbol period, T_S, or decrease the temporal variance, σ^2, of the concurrent transmitters.

3.5 CONCLUSIONS ON THE BASEBAND ANALYSIS

To summarize, a conservative (worst-case, CT received with equal power) threshold is obtained:

$$\Delta t_{eq} \leq \frac{T_S}{2} \tag{3.9}$$

The most useful insight of this chapter is that, when designing communication systems that rely on CT, a tight synchronization is key:

A. Software in the transmitters must be low-level designed to trigger all the CT at the same time; ideally after running exactly the same number of instructions from a common synchronization point used as reference, usually a packet received immediately before, as we will see in real protocols in Chapters 6 and 7.

B. Operating frequencies of the transmitter elements (i.e. microcontroller and radio transceiver) must be high enough and stable enough to make it feasible to operate below the required threshold. Furthermore, different jitter sources, like the variable time usually required by a radio transceiver to decode a packet depending on its power, must be taken into account.

C. If the elements of the transmitters are not able to comply with the requirements, communication bitrate can be decreased to ease the timing demands.

The baseband analysis is an analytical tool useful to roughly understand CT and the impact of synchronization errors in the performance. Nevertheless, it fails to predict the extremely poor behavior experienced using coherently-detected phase modulations in uncoded communication systems, i.e. no spread spectrum or other coding techniques are used. For this reason, in Chapter 4, we need to complement the timing requirements, obtained in baseband, with the power requirements, obtained by analyzing wave interference between concurrent (non-coherent) carriers, which have unavoidable frequency and phase differences.

4

EFFECT OF THE CARRIER IN CONCURRENT TRANSMISSIONS

In Chapter 3, we analyzed the impact of time displacements between CT in the baseband domain, removing the high-frequency carrier effects. As we discuss in this chapter, when severe distortion caused by several carriers sending the same bitstream simultaneously is taken into account, the baseband domain analysis is no longer accurate. Baseband analysis provides a meaningful insight about the importance of tight time synchronization in order to allow proper demodulation, but fails to address the real causes and the main sources of interference. While a baseband analysis can provide some information for trivial non-coherent Amplitude-Shift Keying (ASK) modulation/demodulation schemes, like On-Off Keying (OOK) with envelope detection, it is not enough for phase modulations like BPSK or QPSK. Due to the impossibility of controlling the phase relationships between the concurrent radio waves at the receiver side, and its mostly random nature, there is no longer constructive interference, but an amplitude distortion that appears as a harmful interference. In this case, the time displacement is not the dominant factor, but the power of the strongest received signal compared to the sum of the powers of the other concurrent signals.

We begin considering two concurrent transmitters, with slightly different carrier frequencies (f_{c1} and f_{c2}) and different transmission powers (P_{T1} and P_{T2}), as shown in Fig. 4.1. Differences in the transmission power are used to model relative power differences upon reception of both signals, which can be caused by different path losses or different output powers in the modulators.

Firstly, we analyze the properties of interfering non-coherent waves (Section 4.1) and the resultant beating effect (Section 4.2). Then, we study the impact of having multiple sources and the scalability issues it imposes (Section 4.4).

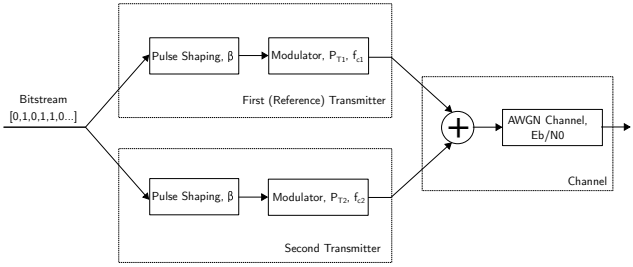

Figure 4.1: Proposed communication system for the high-frequency analysis of two concurrent transmitters

4.1 INTERFERENCE BETWEEN NON-COHERENT WAVES

Independent radio transmitters, even when tightly synchronized, are sources of non-coherent waves: their phase difference is not constant over time. This is due to several unavoidable causes:

A. The carrier in different radio transmitters is generated by different local oscillators, which never have exactly the same frequency, due to its finite accuracy, measured in parts per million (ppm).

B. Independent local oscillators are not synchronized, so they never transmit with a fixed phase relationship.

C. Radio waves coming from different transmitters travel different paths to the receiver, which further results in non-constant (random) phase differences.

All these effects create a fading multipath-like environment that distorts the communication and greatly increases the BER. There are, however, important differences between the effect of multipath receptions and CT:

A. In multipath, all the interfering waves are generated by the same oscillator, so they have the same frequency. In CT frequencies are slightly different, what creates a periodical amplitude distortion.

B. In multipath, phase relationship between the interfering waves can be explained by analyzing differences in path lengths and reflections. In CT phase relationship is mostly random, due to different unsynchronized and independent incoherent oscillators generating the transmissions.

C. In CT the different times of arrival of the concurrent signals are not only due to different propagation times, but also due to temporal misalignments (synchronization errors) between the concurrent transmitters, which can be potentially much higher, even if the transmitters are closely located.

D. In CT, the path that the different signals take to arrive at the receiver, and the channel distortion and attenuation they suffer, can be very different, and depends on the positioning of the different transmitters relative to the position of the receiver. Consequently, there can be big energy (and distortion) dissimilarities between the concurrent signals.

As a result, it is of great interest to analyze the effect of CT in the BER, since a unique phenomenon appears: the beating effect.

4.2 IMPACT OF FREQUENCY DEVIATIONS: BEATS

Beats are known as the interference pattern between two sounds of slightly different frequencies, perceived as a periodic variation in volume whose rate is the difference of the two frequencies. When two waves of similar frequency interfere, there is an alternating temporal pattern of constructive and destructive interference, resulting in the characteristic effect. However, it is not exclusive of sound waves, the same effect appears when electromagnetic waves interfere.

Beats are the dominating phenomena in CT, since the frequency of the interfering waves is slightly different due to small inaccuracies in the local oscillators (Fig. 4.2):

$$f_{c1} \approx f_{c2} \approx f_c \tag{4.1}$$

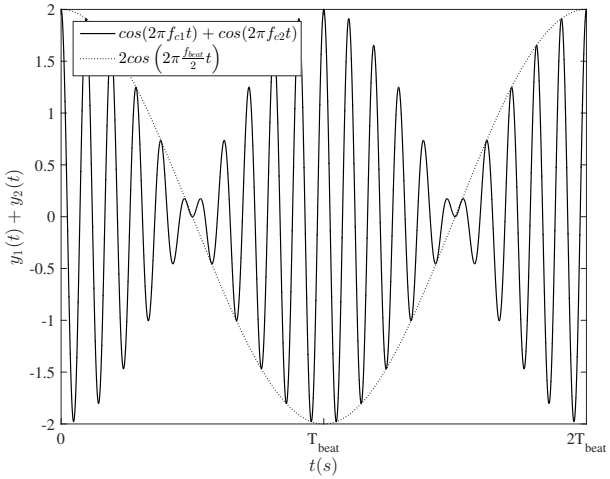

Figure 4.2: Interference between two signals with slightly different frequency: beats ($SIR = 0\ dB$)

$$f_{beat} = |f_{c1} - f_{c2}| \tag{4.2}$$

$$\cos(2\pi f_{c1}t) + \cos(2\pi f_{c2}t) = 2\cos\left(2\pi\frac{f_{c1} + f_{c2}}{2}t\right)\cos\left(2\pi\frac{f_{beat}}{2}t\right) \tag{4.3}$$

As seen in Eq. 4.3, the effect is a wave whose amplitude is modulated with a lower frequency cosine term, known as the envelope. A phase discontinuity of π radians is observed at the zero-crosses of the envelope. As we are considering antipodal phase modulations, like BPSK or QPSK, the phase jump makes it challenging to reliably detect the phase of the incoming wave; particularly for coherent detectors that try to recover the original carrier during the preamble and lock to it for the rest of the transmission. When both transmissions have the same energy, the phase discontinuity provokes a phase jump during half of the

beating period. The consequence is that half of the time the bit is wrongly decoded, even without external noise:

$$BER_{SIR=0dB,BPSK} = 0.5 \tag{4.4}$$

To analyze the effect we assume that, in real-world scenarios, both signals never arrive at the receiver with exactly the same power. To evaluate the impact of concurrent modulated carriers in the receiver performance, we introduce the concept of Signal-to-Interference Ratio (SIR) [57], the ratio between the power of the reference signal and the N interfering signals:

$$SIR = \frac{A_1^2}{\sum_{i=2}^{N} A_i^2} \tag{4.5}$$

As said in Chapter 3, assuming small temporal displacements ($\Delta t < T_S$), most receivers are able to improve their performance by synchronizing with the strongest signal, so for the case of two concurrent transmitters, we can assume that $SIR \geq 0$, what for BPSK can be expressed as:

$$y_1(t) = A_1 \cos(2\pi f_{c1} t + \pi(1 - n(t))); \; n \in \{0, 1\} \tag{4.6}$$

$$y_2(t) = A_2 \cos(2\pi f_{c2}(t - \Delta t) + \pi(1 - n(t))); \; n \in \{0, 1\} \tag{4.7}$$

$$SIR_{2\,Transmitters} = \frac{A_1^2}{A_2^2} \geq 0 \tag{4.8}$$

As seen in Fig. 4.3 and Fig. 4.4, as the SIR is increased the phase distortion decreases and the demodulation becomes feasible.

4.3 POWER AND TEMPORAL DIFFERENCES IN PHASE MODULATIONS

To analyze the effect of this distortion, we perform Monte Carlo simulations with MATLAB, including the beating effect (Section A.1) for different noise levels (E_b/N_0) and different levels of interference (SIR). A pair of square-root-raised-cosine matched digital filters with $\beta = 0.25$ are included in the simulation, as in Chapter 3, to limit the transmission bandwidth, smoothing the signals. Further details about the BPSK CT-baseband model are given in Appendix A.

We define the energy per bit to noise power spectral density ratio (E_b/N_o), as the ratio between the energy of one of the dominant transmitter and the noise. Assuming A_1 referenced to a unit resistor, E_b/N_ocan be defined as:

$$\frac{E_{b\ BPSK}}{N_0} = \frac{(A_1)^2}{2N_0} T_S \tag{4.9}$$

The theoretical BER that we will use, as a reference, is given by the following expression [48]:

$$BER_{1\ Transmitter\ BPSK} = Q\left(\sqrt{\frac{2E_b}{N_0}}\right) \tag{4.10}$$

It is the same expression as the one used for the antipodal baseband system in the previous chapter (Eq. 3.3). The simulations are performed with BPSK, but the results can be extended to QPSK, OQPSK and coherently detected MSK, since they have similar constellations and, therefore, similar performance in AWGN channels.

The results of Fig. 4.5 and Fig. 4.6 are obtained. Not only no gain is experienced because of the existence of CT, but, on the contrary, the interference is extremely destructive, particularly for this type of modulation, where the information is codified in the

phase of the wave and coherently demodulated. Only for SIR levels greater than 20 dB the communication performance resembles that of only one transmitter.

Several considerations must be taken into account:

A. Differently from the ideal baseband scenario, described in Chapter 3, at the frequency of the carrier and with phase modulations, the time displacement, Δt, between the concurrent signals loses relevance; since small differences in frequency and transmission paths greatly distort the phase of the received signal, rendering any synchronization attempt ineffective.

B. As intuitively expected, when the SIR equals 0 dB, BER is 0.5 (Eq. 4.4), as we receive two signal with the same power, which have a completely random phase relationship, that even changes over the time due to the beating effect. Bit information is completely destroyed by the alternating positive and negative cycles of the envelope, they introduce time varying phase ambiguity.

C. Demodulation of every bit is considered independent, apart from the low Intersymbol Interference (ISI) introduced by the raised-cosine pulse shaping. In a real demodulation system, bits are transmitted within the context of a packet. Techniques, such as as using a well-known preamble, further help resolving phase ambiguity. This is particularly true with channel coding, such as Direct Sequence Spread Spectrum (DSSS), able to effectively decrease interference due to CT [57].

D. At every zero cross of the envelope, which happens at a rate equal to the beating frequency, a phase inversion takes place if the SIR is close to zero. As we will see in Section 5.3, SIR tends to zero in the presence of multiple concurrent transmitters. Mechanisms able to cope with these bit inversions, while a packet is being received (like midambles), are needed to effectively demodulate the signal. Since normally a packet reception spans several beating periods, an unique

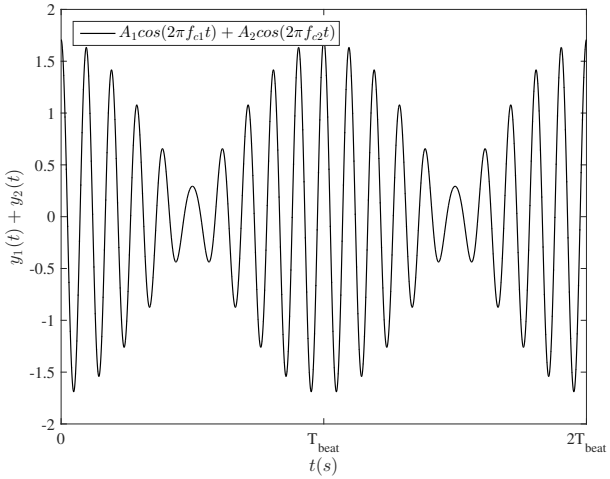

Figure 4.3: Interference between two signals with slightly different frequency: beats ($SIR = 3\ dB$)

phase estimation during the preamble is not enough, and will not hold during the reception of the packet.

4.4 MULTIPLE CARRIERS INTERFERING: SCALABILITY ISSUES

Based on the MATLAB simulation performed in Section 4.2, a threshold to reasonably limit the losses caused by two CT in coherently-detected antipodal phase modulations can be established as:

$$SIR_{Min\,BPSK} = 20dB \tag{4.11}$$

Using the Friis Transmission Equation, we can derive the maximum allowed density of transmitters:

$$\frac{P_R}{P_T} = G_T G_R \left(\frac{\lambda}{4\pi d}\right)^2 \tag{4.12}$$

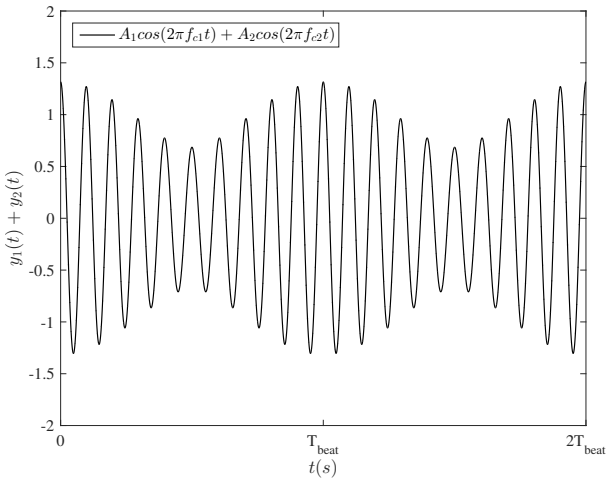

Figure 4.4: Interference between two signals with slightly different frequency: beats ($SIR = 10\ dB$)

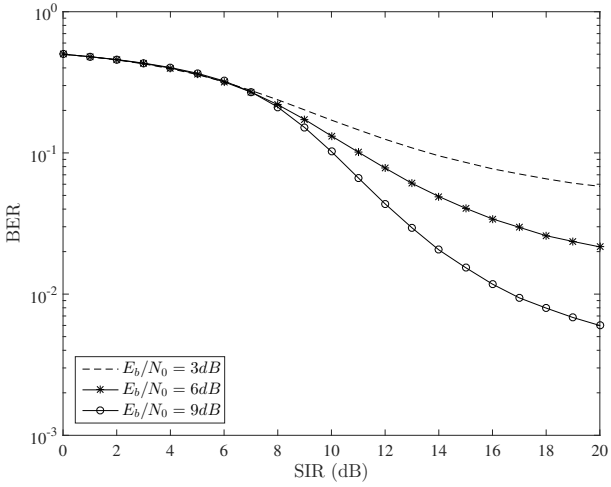

Figure 4.5: BER for two concurrent transmitters with different noise levels and SIR (BPSK, I)

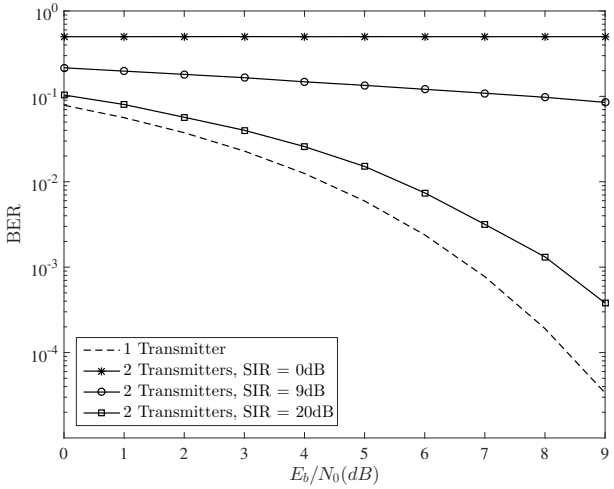

Figure 4.6: BER for two concurrent transmitters with different noise levels and SIR (BPSK, II)

where:

- $P_{R,}P_T$: powers at the receiving and transmitting sides, respectively.
- $G_{R,}G_T$: gains of the receiving and transmitting antennas, respectively.
- λ: wavelength.
- d: distance between the transmitting and receiving antennas.

Applying Eq. 4.12 for the situation of two concurrent transmitters and assuming that:

A. Antennas are in far field and unobstructed free space.

B. Bandwidth is narrow enough so that a single wavelength can be assumed.

C. Antennas are correctly aligned and polarized.

D. Gains of the concurrent transmitting antennas are equal ($G_{T1} = G_{T2} = G_T$).

E. Transmission power of the concurrent transmitters is the same ($P_{T1} = P_{T2} = P_T$).

We can then calculate the relationship between distances d_1 and d_2:

$$\frac{P_{R1}}{P_T} = G_T G_R \left(\frac{\lambda}{4\pi d_1}\right)^2 \tag{4.13}$$

$$\frac{P_{R2}}{P_T} = G_T G_R \left(\frac{\lambda}{4\pi d_2}\right)^2 \tag{4.14}$$

where:

- d_1: distance between the first transmitting antenna and the receiver.
- d_2: distance between the second transmitting antenna and the receiver.

Dividing Eq. 4.13 and Eq. 4.14, and imposing condition of Eq. 4.11, we obtain:

$$\frac{P_{R1}}{P_{R2}} = \left(\frac{d_2}{d_1}\right)^2 \tag{4.15}$$

$$10\log\left(\frac{P_{R1}}{P_{R2}}\right) = 20\log\left(\frac{d_2}{d_1}\right) \geq 20dB \tag{4.16}$$

The second transmitter must be, approximately, ten times further than the first, dominant, transmitter:

$$d_2 \geq 10 d_1 \tag{4.17}$$

This result is a proof of the poor performance of CT with simple coherently-detected phase modulation systems. Packet reception is only possible if there exists a dominant signal, stronger than the sum of the other simultaneous transmissions. In case there are more than two transmitters, d_2 can be seen as the distance from the receiver to a transmitters that would be received with the same power as the sum of all the CT that compete with the strongest one. The need for single predominant transmissions completely breaks system scalability, rendering the use of CT ineffective in real scenarios with flexible topologies.

Losses may be mitigated introducing some degree of smart power control, increasing energy diversity; but performance, in general, is expected to be poor in phase-modulated communication systems, using CT with coherent detectors; since the transmission is very distorted due to the beating effect. With these conditions, coherent detection using carrier recovery techniques is ineffective, since the signal at the receiver no longer has a fixed phase and frequency that can be recovered to efficiently demodulate the transmission, at least without further information, such as fixed patterns within the packet (like a preamble).

4.5 CONCLUSIONS ON THE CARRIER EFFECT

After the optimistic results of the baseband analysis of Chapter 3, where the problem was reduced to a feasible synchronization matter, in this chapter we demonstrate that CT do not work as expected in real (carrier-based) communication systems.

The following conclusions can be remarked:

a. CT appear as a very harmful interference (much more than uncorrelated AWGN) for coherently-detected phase modulations, due to the strong phase distortion caused by the beating effect. An attempt to synchronize the concurrent transmitters to constructively interference would fail at practical frequencies, since the short wavelength of the carrier would require an extremely accurate clock (in the order of hundredths of nanoseconds for gigahertz communications). Furthermore, different propagation times and paths from

the transmitters to the receivers would also need to be compensated, rendering the effort impractical, if even achievable.

B. CT in coherently-detected phase-modulated communication systems only work for low-density networks, where a dominant transmission can be detected by every receiver, and does not scale. Power control techniques can improve the situation, but not greatly without complicating the protocol, removing the main advantage of using CT over routing mechanisms: simplicity.

C. Receiver features have a critical impact, being automatic gain control and dynamic frequency offset compensation during receptions of great importance for CT to work; ideally carrier recovery systems should be able to deal with quickly oscillating amplitudes and frequencies (due to the beating effect). As a rule of thumb, receivers performing well in multipath conditions are good candidates for CT-based communication systems. Also, proper channel equalization, as in multipath environments, can mitigate the distortion.

D. Differential Phase-Shift Keying (DPSK), used in conjunction with non-coherent detection, is a better alternative if phase modulation is a requirement. Since the received signal is a superposition of multiple sinusoidal waves, each of different amplitude and phase, phase discontinuities are, ideally, only observed in instants multiple of the sample period; assuming that all concurrent transmitters are well synchronized. A simple, non-coherent detector, can use these discontinuities to identify the boundaries of the symbol periods, and use the previous symbol as a template to distinguish between different bits. In this case, since we do not have to recover the carrier in the receiver, the main distortion is in the amplitude of the wave. However, the performance is still poor, and further channel coding and recovery techniques, such as DSSS paired with soft-decision decoding are still needed to limit the packet error rate [38]. Further-

more, additional phase discontinuities may appear at the zero crosses of the envelope, complicating the synchronization with the symbol period and periodically inverting the phase references for the bits.

The analysis helps us to realize the non-coherent nature of CT-based communication systems and one important insight: non-coherent receivers are the natural choice. Furthermore, since the beating effect greatly distorts the phase and amplitude of the received wave, frequency modulations are the way to go.

To overcome these heavy limitations, we need to introduce different modulation techniques. In Chapter 5, we will focus on CT-friendly modulation techniques: those in which the information is codified in the frequency of the carrier, particularly when demodulated with simple energy detectors. We will analyze how non-coherent receivers, like FSK with envelope detection, can cope with CT more efficiently than simple coherent phase modulations.

5

UNDERSTANDING CONCURRENT TRANSMISSIONS: CAPTURE AREA

In the previous chapter, we explained how introducing the wave interference effects that happen when concurrent carriers interfere can dramatically affect the performance, degrading the BER results from those obtained in baseband. The main difference is the beating effect, appearing as an alternating pattern of constructive and destructive interference. Under these circumstances, coherent modulations might fail to effectively recover a precise local carrier, needed to decode the transmitted bitstream.

Real receivers use expected patterns to solve phase ambiguity, but normally only during the reception of the packet preamble. Phase discontinuities can further appear in the middle of a symbol reception, due to the arrival of a stronger transmission, while synchronized with a weaker one, or due to the beating effect when all the transmitters are received with similar energy ($SIR \approx 0\ dB$), what happens when there are a lost of concurrent transmitters (Section 5.3). The ability to cope with the beating period, and the periodic phase jumps it might cause, is key.

Even when modern coherent receivers may work relatively well in the presence of CT, we are not using their advantages, since they are working in a harsh environment that they were not designed for. A more efficient alternative is using simpler, non-coherent receivers and, even, energy-efficient frequency modulations. Amplitude and phase properties are not well preserved when multiple waves, with slightly different properties, simultaneously interact and arrive at the receiver. Frequency has a more robust behavior, particularly if the demodulation is based on simple band-pass filtering and envelope detection, which offers some tolerance to frequency deviations and simply compares measured energy in orthogonal frequency bands. One example is the non-coherent Binary Frequency-Shift Keying (BFSK) receiver (Fig. 5.1).

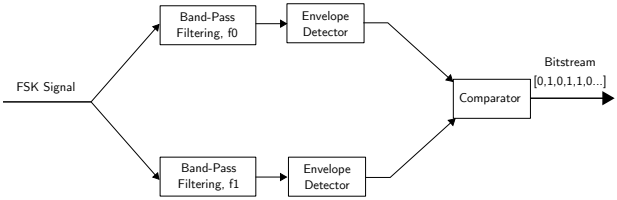

Figure 5.1: Non-coherent BFSK receiver

Firstly, we introduce the BFSK model that we will use throughout the chapter (Section 5.1). Then, the performance of the modulation is evaluated with two concurrent transmitters (Section 5.2), as done in previous chapters. The important concept of capture area is presented in Section 5.3, and calculated for typical modulations. Finally, a comprehensive scalability analysis is given in Section 5.4.

5.1 SURVIVING THE BEATING EFFECT WITH FREQUENCY MODULATIONS

First of all, as we did for BPSK in Chapter 4, we define two concurrent BFSK transmitters, with a relative temporal displacement, Δt, different amplitudes, A_1 and A_2, and slightly different carrier frequencies, $f_{c1}$and f_{c2}, sending an antipodal bitstream, n, with the following equations:

$$y_1(t) = A_1 \cos(2\pi(f_{c1} + n(\Delta f_1))t);\ n \in \{-1, +1\} \tag{5.1}$$

$$y_2(t) = A_2 \cos(2\pi(f_{c2} + n(\Delta f_2))(t - \Delta t));\ n \in \{-1, +1\} \tag{5.2}$$

$$f_{c1} \approx f_{c2} \approx f_c \tag{5.3}$$

$$\Delta f_1 \approx \Delta f_2 \approx \Delta f \tag{5.4}$$

$$f_{beat} = |f_{c1} - f_{c2}| \tag{5.5}$$

$$SIR_{2\,Transmitters} = \frac{A_1^2}{A_2^2} \geq 0 \tag{5.6}$$

For illustrative purposes, we choose the following parameters, being T_S the symbol (bit) period:

$$f_{beat} = \frac{1}{4T_S} \tag{5.7}$$

$$\Delta f = \frac{1}{2T_S} \tag{5.8}$$

And the modulation index, h, is defined as:

$$h = 2\Delta f T_S = 1 \tag{5.9}$$

This is the minimum modulation index for non-coherent orthogonal detection [52].

We see the differences between the signal of only one transmitter (Fig. 5.2) and the resultant beating waveform from the interference of two concurrent transmitters (Fig. 5.3). As a first insight, we observe how the resultant distortion affects mostly to the amplitude and phase of the wave, leaving the frequency differences (due to the bit modulation) still visible. As we will see in the following sections, this translates to a much better performance of non-coherent BFSK over coherent BPSK, since the bit information is better preserved in the presence of CT.

As demodulator, we use a simple non-coherent energy detector, since it provides some advantages over coherent operation; particularly, there are no requirements for accurate phase recovery in the receiver, what can be tricky due to the beating waveform, and

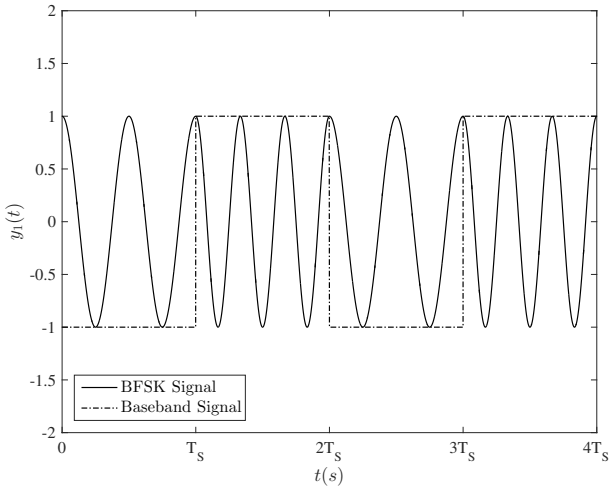

Figure 5.2: Modulated BFSK signal (1 Transmitter)

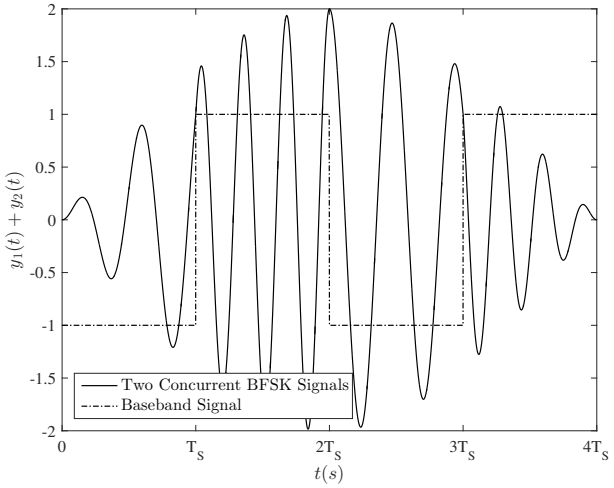

Figure 5.3: Interference between two BFSK signals with slightly different frequencies: beats ($SIR = 0\ dB$, $\Delta t = 0$)

adds complexity to the whole system. Furthermore, the main advantage of coherent detection (better AWGN rejection) is already provided by the usage of CT, since the noise is effectively removed when multiple transmissions combine their energy (Section 5.4).

The theoretical BER that we will use, as a reference, is given by the following expression (non-coherent detection of orthogonal BFSK [48]):

$$BER_{1\ Transmitter\ BFSK} = \frac{1}{2}\exp\left(-\frac{E_b}{2N_0}\right) \tag{5.10}$$

It is the expected performance of non-coherent orthogonal BFSK detection in the presence of AWGN noise. In the following sections, we will evaluate how CT degrade this performance.

5.2 POWER AND TEMPORAL DIFFERENCES IN FREQUENCY MODULATIONS

First of all, we analyze how two perfectly synchronized ($\Delta t = 0$) concurrent transmitters perform in AWGN channels, in comparison to one transmitter (Eq. 5.10), by varying their relative power levels (SIR). The temporal waveforms can be seen in Fig. 5.3 ($SIR = 0\ dB$), Fig. 5.4 ($SIR = 3\ dB$) and Fig. 5.5 ($SIR = 10\ dB$). Except from the amplitude distortion, which makes the signal more sensitive to noise, frequency properties are mostly preserved.

As we did in previous chapters, to quantitatively analyze the effect of the distortion, we perform Monte Carlo simulations with MATLAB, including the beating effect (Section A.2) for different noise levels (E_b/N_0) and SIRs. Further details about the BFSK CT-baseband model are given in Appendix A. The results are presented in Fig. 5.6 and Fig. 5.7. Only for $SIR = 20\ dB$, we appreciate the characteristic waterfall-like curve of the BER vs E_b/N_0, being the error reduction much flatter for lower SIR, as is the case in communication systems suffering from related effects, like multipath channel fading (Section 2.2). In Section A.2 and Fig. A.7, the same BER curve is analytically obtained for the most simple

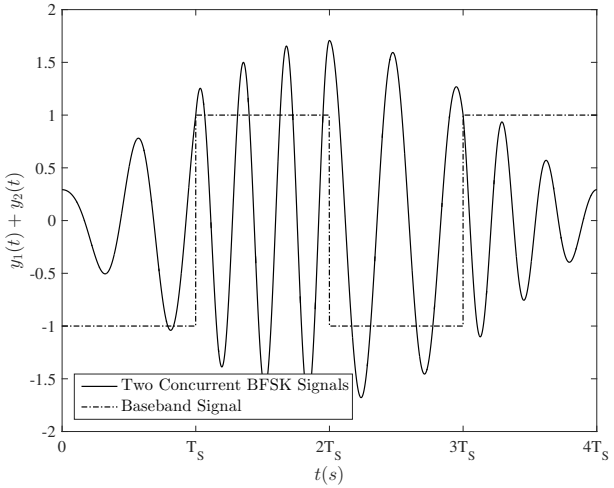

Figure 5.4: Interference between two BFSK signals with slightly different frequencies: beats ($SIR = 3\ dB$, $\Delta t = 0$)

case ($\Delta t = 0$ and $SIR = 0\ dB$), validating the accuracy of the performed simulations.

It is interesting to remark that, while in the coherent BPSK system of Section 4.2 the BER always decreases when increasing the SIR; now, with non-coherent BFSK, we can differentiate between two regions:

A. Roughly in the region $0\ dB \leq SIR \leq 8\ dB$, the BER increases when increasing the SIR.

B. For $SIR \geqslant 8\ dB$, the BER starts decreasing again, and converges to the BER value for only one transmitter:

$$BER_{2\ Transmitters\ BFSK}(SIR \to \infty) = \frac{1}{2} \exp\left(-\frac{E_{b\ FSK}}{2N_0}\right) \quad (5.11)$$

It is important to remember that E_b/N_0 is calculated referenced the energy of only one (the dominant) transmitter. Assuming A_1 referenced to a unit resistor, $E_b/N_o$for our BFSK system can be defined as:

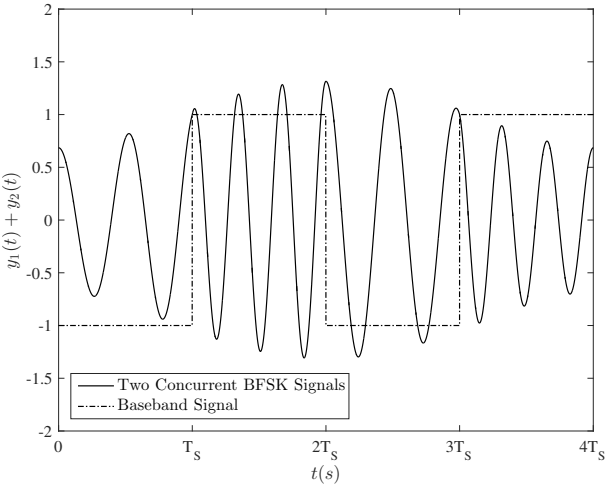

Figure 5.5: Interference between two BFSK signals with slightly different frequencies: beats ($SIR = 10\ dB$, $\Delta t = 0$)

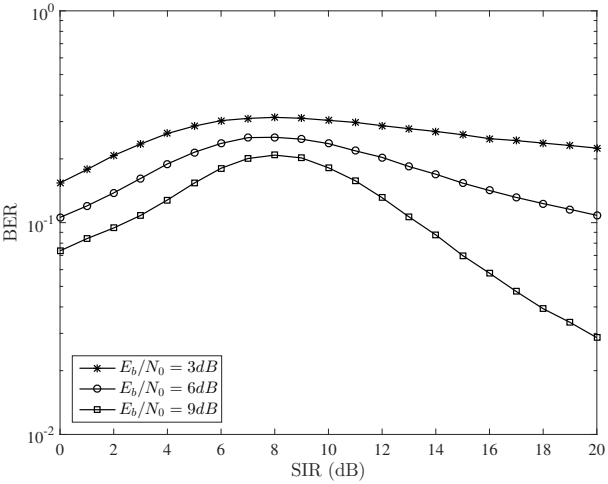

Figure 5.6: BER for two concurrent transmitters with different noise levels and SIR (BFSK, $\Delta t = 0$, I)

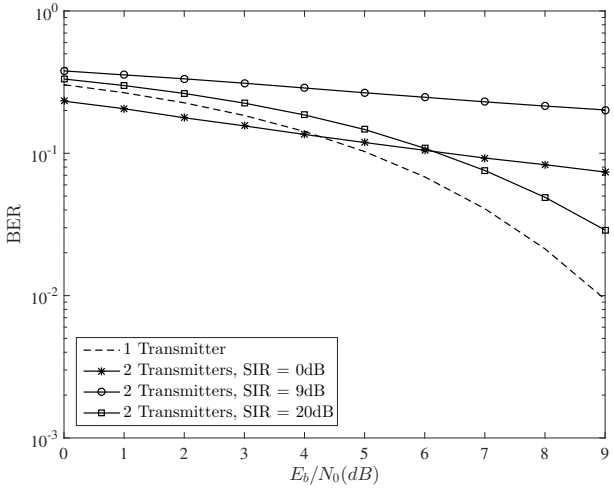

Figure 5.7: BER for two concurrent transmitters with different noise levels and SIR (non-coherent BFSK, $\Delta t = 0$, II)

$$\frac{E_{b\ BFSK}}{N_0} = \frac{(A_1)^2}{2N_0} T_S \tag{5.12}$$

Thus, with this definition, adding the energy of the second transmitter (proportional to A_2), a gain in the performance against noise can be expected in some conditions: when the positive effect of constructive interference surpasses, in average, the distortion of destructive interference. To further analyze the effect, we plot the results of multiple simulations for multiple (SIR, E_b/N_0) pairs, obtaining the Fig. 5.8, defining the *Gain* as the ratio between the energy of the dominant transmission to the energy of a single transmitter with the same BER performance (using Eq. 5.10):

$$Gain = \frac{-2\ln(2BER_{2\ Transmitters\ BFSK})}{E_{b\ FSK}} \tag{5.13}$$

The following conclusions are obtained (Fig. 5.8):

A. Only for a SIR close to 0 dB, and noisy receptions ($E_b/N_0 < 3dB$), a gain in the performance (peaking around 3 dB) is

observed using two concurrent transmitters instead of one (red region in Fig. 5.8).

B. In general, a decreased performance is experienced (blue area in Fig. 5.8), reaching losses of about 6 dB in low-noise scenarios.

With $SIR = 0\,dB$, we are spending 3 dB more energy by sending with two transmitters. A constant gain of 3 dB would be desirable, to be energy efficient and equal the performance of a single transmitter sending with double the energy. But this is only the case in the high-noise region.

It is useful to define the energy efficiency of CT as (Figure 5.11):

$$Efficiency = \frac{Gain}{1 + \frac{E_b[y(2)]}{E_b[y(1)]}} = \frac{Gain}{1 + \frac{(A_2)^2}{(A_1)^2}} \tag{5.14}$$

An efficiency of 100% means that the BER of the two CT is equal to that of a single transmitter sending with the same energy. It happens when the higher BER during destructive interference periods is compensated by the lower BER during constructive interference periods. Efficiencies higher than 100% can be observed in some channel models, since during the constructive interference phases the received signal achieves highly energetic periods (twice as energetic as sending with only one transmitter with double the energy).

But this is not the case for the assumed AWGN channel in the simulated range. Only for low SIR and high noise, or high SIR (which becomes close to sending with only one transmitter), the energy efficiency is similar to sending with only one transmitter with equal combined energy (efficiency close to 100%). This might give the impression that CT-based protocols are not energy efficient, and it is true for two (or a low) number of transmitters; neglecting other diversity effects (like spatial diversity). Nevertheless, when using a higher number of transmitters, CT unlock their potential, and higher efficiencies are actually observed in very noisy scenarios. This is particularly true when power limitations of individual transmitters (due to regulations and design

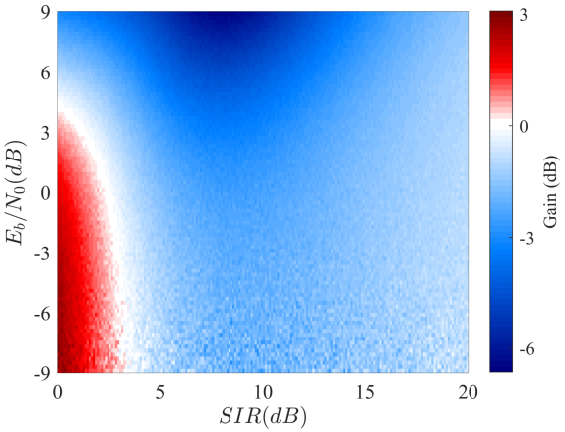

Figure 5.8: Gain for two concurrent transmitters (compared to one transmitter) with different noise levels and SIR (non-coherent BFSK, $\Delta t = 0$)

constraints) make it infeasible to equal the combined energy of multiple CT with only one node, and the noise is too strong to effectively communicate with the energy of a single transmitter. Furthermore, the usage of CT not only brings energy efficiency, but also simple latency-optimal mesh network protocols, as discussed in Part iii. A further analysis about the energy efficiency, with a higher number of concurrent transmitters is performed in Section .8.4

Now, we will show how temporal displacements, Δt, further affect the BER. Fixing the relative power of both transmitters ($SIR = 20\ dB$), we gradually desynchronize them, and repeat the MATLAB simulations, obtaining the results of Fig. 5.10 and Fig. 5.11. As expected, as the displacement becomes closer to the symbol period, T_S, the BER greatly increases due to the temporal overlap of different symbols.

Both power and temporal differences greatly affect and determine the performance of the communication system in the presence of CT. To analyze the combined effect of both variables (Δt

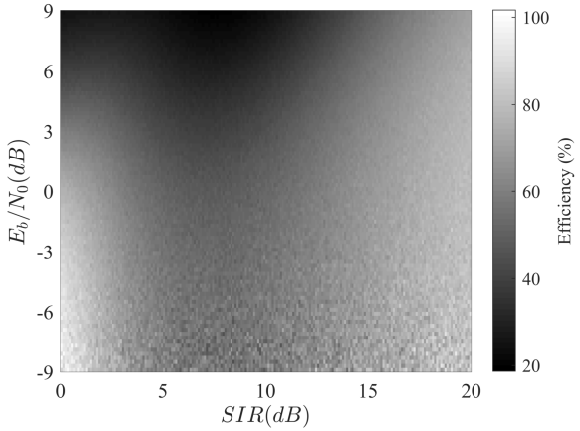

Figure 5.9: Efficiency for two concurrent transmitters (compared to one transmitter) with different noise levels and SIR (non-coherent BFSK, $\Delta t = 0$)

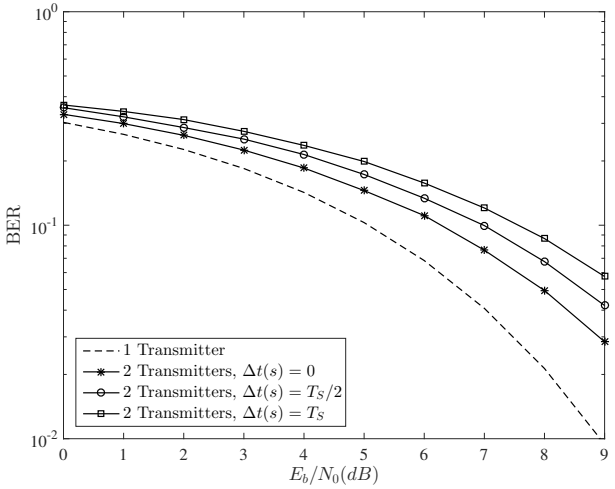

Figure 5.10: BER for two concurrent transmitters with different noise levels and time displacements (non-coherent BFSK, $SIR = 20\ dB$, I)

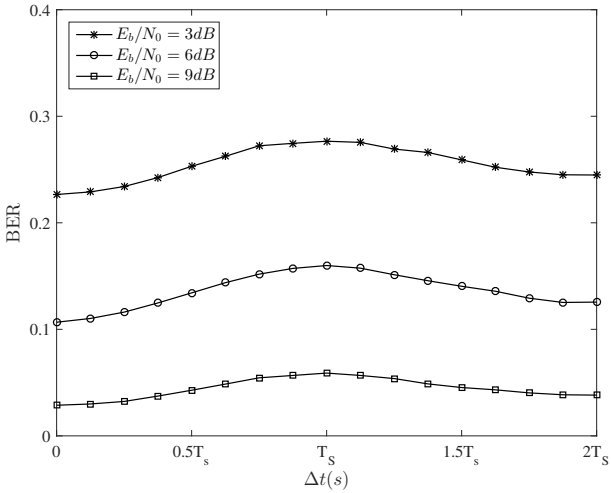

Figure 5.11: BER for two concurrent transmitters with different noise levels and time displacements (non-coherent BFSK, $SIR = 20\ dB$, II)

and SIR), we introduce in the next section the concept of capture area.

5.3 COMBINING TEMPORAL AND POWER EFFECTS: CAPTURE AREA

We still require a tool to easily visualize if CT can be used in a particular communication system, with a defined modulation. To fill this gap, we introduce the concept of capture area, defined as:

the BER obtained as a result of the interference between two concurrent transmitters, in the absence of noise, in the two-dimensional region defined by $-3\ dB \leq SIR \leq 3\ dB$ *and* $0 \leq \Delta t \leq 0.5T_S$.

We will use the capture area, as a figure of merit, to characterize the performance of communication systems in the presence of CT. The negative SIR region is understood as the error rate that the demodulator would experience in the theoretical case it synchronizes with the weakest signal.

We calculate the capture area for different modulations, using MATLAB simulations and their CT-baseband equivalent model (Appendix A). Varying both the time displacement, Δt, and the SIR, we obtain three-dimensional figures, represented here as two-dimensional gray-scale pictures, for simplicity:

A. *Baseband with rectangular pulses* (Fig. 5.12). In the ideal baseband scenario (Section 3.1), we can see how for every $SIR > 0\ dB$, the BER is 0, as expected; since the demodulator is synchronized with the strongest signal and the interference introduced by the second transmitter is not enough to produce a bit inversion. For $SIR < 0\ dB$, the demodulator is synchronized with the weakest signal, and poor performance is observed if the time displacement is big enough ($\Delta t \geq 0.5T_S$). Inside the capture area, the error is zero.

B. *Baseband with pulse shaping* (Fig. 5.13). With pulse shaping (Section 3.2) the results are very similar to those in the previous case, but the regions appear smoothly, with the hard transitions removed. The error performance is still optimal (zero) inside the defined capture area.

C. *Coherently-detected BPSK, QPSK, OQPSK or MSK with pulse shaping* (Fig. 5.14). For the BPSK system of Section 4.2, the demodulator is not able to properly recover the phase of the incoming carrier and demodulate the transmission in the presence of strong beating. The BER is practically maximum (0.5, random behavior) until the beating effect is minimized increasing the SIR. The BER does not depend on the time displacement, since the simultaneous transmission appears as noise, and has a random phase relationship with the reference signal, as both transmitters feature non-coherent oscillators. The error performance is extremely poor (0.5 error rate) inside the capture area. This case shows a situation in which CT are not working, and how the capture area is able to identify it.

D. *Non-coherently detected BFSK with rectangular pulses* (Fig. 5.15). For the BFSK system of Section 5.1 (rectangular pulses), featuring non-coherent detection, the results are similar to those

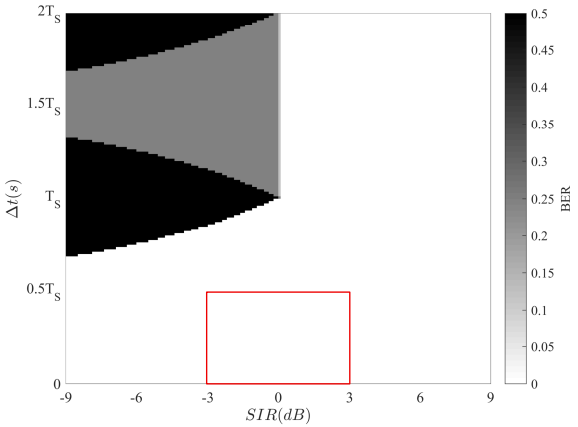

Figure 5.12: Interference between two signals in baseband with rectangular pulses (capture area inside the red rectangle)

obtained in baseband, but with wider error lobes. Hard transitions are observed, since no pulse shaping is considered. In the capture area, the error is again zero, since the amplitude distortion of the beating effect is not able to provoke a frequency shifting and invert the bit decision, as is the case with amplitude ad phase the modulations. This is a proof of the natural robustness of frequency modulations in the presence of CT.

A further analysis of the capture area and a summary of the results are presented in Section 8.1.

Although the capture area is derived from the simulation results with only two transmitters, it can be used to obtain the expected outcome with multiple concurrent transmitters:

if the BER is zero or close to zero inside the capture area, the communication system has a good performance (scales greatly) in the presence of multiple concurrent transmitters, assuming the time displacement is below half the symbol period; if the BER is not close to zero inside the capture area, the system is not a good candidate for the usage of CT-techniques (scales poorly).

This can be explained in the following manner:

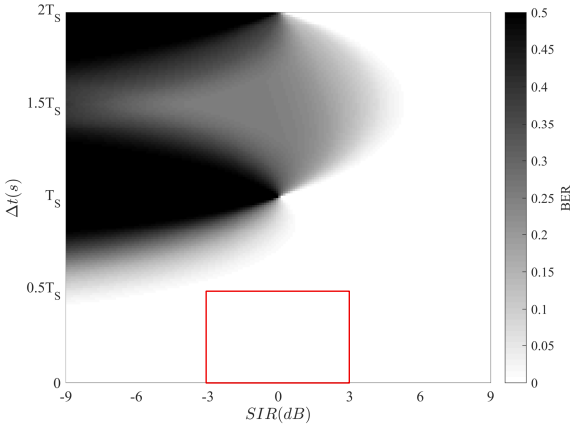

Figure 5.13: Interference between two signals in baseband with pulse shaping (capture area inside the red rectangle)

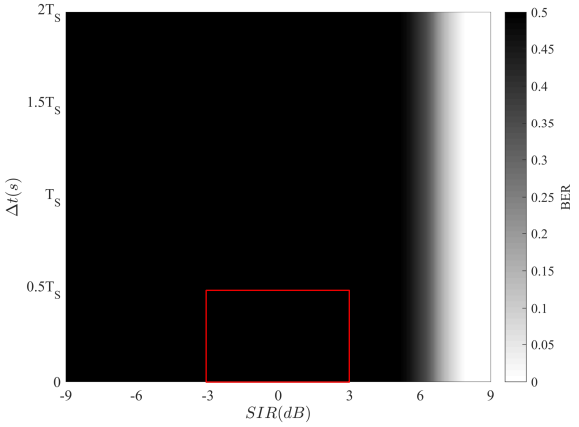

Figure 5.14: Interference between two coherently detected BPSK, QPSK, OQPSK or MSK signals with pulse shaping (capture area inside the red rectangle)

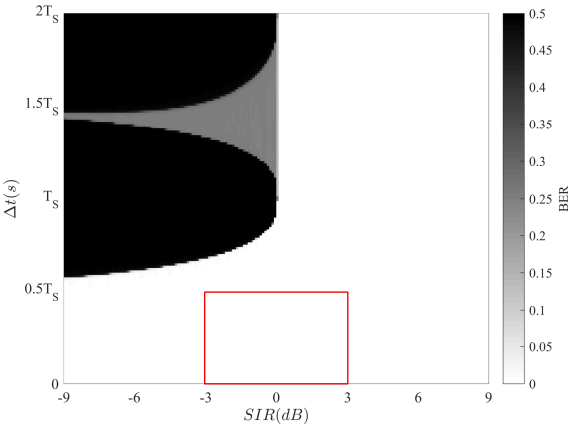

Figure 5.15: Interference between two non-coherently detected BFSK signals with rectangular pulses (capture area inside the red rectangle)

A. In a system with a lot of concurrent transmitters, the receiver will tend to operate in a region around $SIR = 0\ dB$. When there are a large number of CT, it is no longer possible to distinguish between the energy of the main transmission and the interfering energy, since we can no longer define a dominant signal. Deep energy depressions and fluctuations are to be expected:

$$SIR \approx 0\ dB \quad for\ large\ N \tag{5.15}$$

This is why the capture area is defined in $-3\ dB \leq SIR \leq 3\ dB$: a dense CT-based system tends to operate in this region, characterized for a strong amplitude beating. Since we are mainly interested in dense networks, receivers must behave well under these conditions.

B. The condition of $0 \leq \Delta t \leq 0.5T_S$ was obtained in Chapter 3, as a feasible threshold that our system should comply with in order to actually operate in a CT-mode, rightly synchronized, as opposed to a random-access collision-based mode, in which different bits from different transmitters

overlap in the air, destroying the information due to the ISI. In the following section we will analyze how the maximum time displacement condition limits the maximum number of concurrent transmitters.

c. For $\Delta t > T_S$, the situation is similar to that of two independent bitstreams (different packets) colliding in the air. As it can be seen, in BFSK (Fig. 5.15) the error is low as long as the packet of interest is stronger ($SIR > 0\ dB$, in practical scenarios with pulse shaping and noise about 3 dB is a more realistic threshold [37]). This result also demonstrates the applicability of the well-known classical (non CT-based) *capture effect* in frequency modulations (Section 2.2). We also show that the classical *capture effect* does not work in phase modulations, since the performance is still extremely poor in the region $\Delta t > T_S$ (Fig. 5.14).

5.4 SCALABILITY ANALYSIS BASED ON THE CAPTURE AREA

The capture area gives us a useful tool to decide if the communication system works (is scalable) in the presence of CT.

Two conditions must be satisfied:

a. *BER must be close to zero inside the capture area for CT-based systems to scale*. This condition is determined by the working principle of the modulator and demodulator systems (e.g. coherent vs. non-coherent detection, phase-modulation vs. frequency-modulation, etc.). In our Figures, it means that the capture area must be completely white (error-free in the absence of noise), what only happens in the baseband cases (Figures 5.12 and 5.13), and in the non-coherently detected BFSK (Figure 5.15). CT is not working (BER is too high to be considered of practical use) for the analyzed phase modulation (Figure 5.14).

b. *The equivalent temporal displacement, Δt_{eq}, must be below half the symbol period, $T_S/2$.* While the previous condition was mainly fixed by the chosen modulation scheme, and the analytical inspection of the capture area; in this case the actual

implementation of the communication system has a heavy impact. As discussed in Section 3.4, a statistical analysis, considering that the pairwise temporal displacements follow a normal distribution with standard deviation, σ, leads to the following condition regarding the maximum number of concurrent transmitters, N_{max} (Figure 5.16):

$$N_{max} = \left(\frac{T_S}{6\sigma}\right)^2 \tag{5.16}$$

The standard deviation, a property determined by the different hardware and software delays of the transmitters, ultimately defines how dense a CT-based network can be. It addresses the importance of techniques like clock offset compensation and fine tuning of the number of executed instructions in every node [8], as we will see in real protocols in Part iii.

The following consideration is remarked:

the BER of a CT-based system with multiple transmitters resembles the BER inside the capture area, given a large enough number of concurrent transmitters (so that the SIR tends to zero and the noise can be neglected); but not too large to keep the equivalent temporal displacement below half the symbol period:

$$2 \ll N_{Capture\ Area} \leq N_{max} \tag{5.17}$$

And this imposes a condition in the standard deviation (temporal jitter) of the individual transmitters:

$$\sigma \ll \frac{T_S}{6\sqrt{2}} \tag{5.18}$$

When designing a CT-based system, not only suitable modulations and channel coding schemes must be chosen, but also a mechanism to keep the concurrent transmitters tightly synchronized must be provided. If digital clocks in the transmitters are not accurate or stable enough to satisfy the requirements, or the network protocol cannot provide the required synchronization, lower symbol rates can be used to ease the condition.

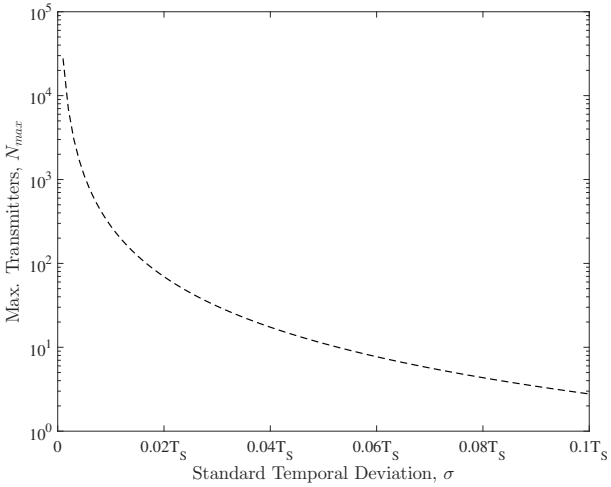

Figure 5.16: Maximum number of concurrent transmitters in CT-based systems (*imposing* $\Delta t < T_S/2$)

5.5 CONCLUSIONS ON THE PERFORMANCE OF FREQUENCY MODULATIONS

The main conclusions obtained after the analysis of CT with frequency modulations are the following:

A. *Non-coherent detection is a better choice*. The beating effect greatly distorts the amplitude and phase of the resultant combined transmission due to the non-coherent addition of different waves with slightly different frequencies and random phase relationships. The natural choice for demodulating beating waves is a non-coherent receiver, given the difficulty of relying on a local carrier recovery system when the properties of the incoming wave are quickly changing (beating). Coherent detection might perform relatively well with modern, agile and robust carrier recovery systems, paired with channel coding techniques, such as DSSS, able to more reliably perform the demodulation in the presence of beating. Nevertheless, the extra cost and complexity of dependable coherent systems are not required with CT.

B. *Frequency modulations are more reliable*. While information codified in the amplitude and/or phase can be tricky to recover in the presence of CT, a simple energy detector tuned to two orthogonal frequencies is perfectly capable of reliably demodulate a multitude of concurrent signals, given the equivalent time displacement is smaller than $T_S/2$ (to limit the ISI).

C. *Great noise rejection*. Dense CT-based systems tend to minimize the effect of AWGN noise, since CT use multiple paths (great diversity) and are combined at the receiver resulting in a highly energetic field. The main loss mechanism is then the internal interference due to the simultaneous transmissions, caused by the destructive interference periods and the ISI due to the temporal misalignments; the effect of the noise is minimized. This is also the reason why the capture area is defined to be obtained without introducing AWGN noise in the simulations, since external interference can be neglected given a large enough number of concurrent transmitters. The cost of noise rejection is the energy used by all the simultaneous transmissions. This feature greatly compensates the classical main disadvantage of non-coherent systems (worse performance in AWGN channels).

Inexpensive and non-coherent FSK energy detectors perform optimally (great noise rejection and scalability) with CT-based flooding protocols; eliminating the need for complex coherent communication systems, which in this scenario can be counterproductive. All the energy used in the redundant transmissions pays off due to the great simplicity of the system, particularly in extremely harsh and noisy environments. The complexity is moved from the modulator/demodulator system to the task of synchronizing all the transmitters to relay the same information (bitstream) within the temporal limits in which CT work ($\Delta t < T_S/2$). In Part iii we will analyze real protocols that use CT, evaluating how they solve the synchronization problem.

Part III

EXPERIMENTAL RESULTS AND VALIDATION

Up to know, we have discussed through theoretical results and simulations how CT, given the right conditions, constitute a powerful mechanism to deploy simple and reliable wireless communication links. Now, we want to validate our results by implementing CT in real-world applications. We present two award winning protocols: RedFixHop and BigBangBus. Both have been successfully tested in challenging scenarios, with mesh networks of arbitrary topology and high interference. RedFixHop is designed to work in one-to-all scenarios, achieving optimal CT by using hardware ACKs; while BigBangBus is an extremely robust, multi-source, many-to-all protocol.

6

REDFIXHOP: RELIABLE ULTRA-LOW LATENCY NETWORK FLOODING

RedFixHop [36][21][19][20][22], a CT-based flooding mechanism, is proposed to achieve highly reliable source-to-sink communication of very short critical packets within a WSN working in harsh environments. RedFixHop's main innovation is the usage of hardware-generated ACKs to propagate the message within the network, without requiring the involvement of the main microcontroller; achieving optimal synchronization, which means greater scalability and easier application programming than current CT-based protocols like Glossy [36] [26]. Acknowledgment (ACK)s are used in a clever and innovative way, to further propagate the packet using flooding and CT techniques, instead of their original purpose (provide confirmation of the packet reception).

As discussed in Part ii, CT are successful only if the senders synchronize their packet transmissions with sub-microsecond precision. In order to achieve the required synchronization accuracy, packet retransmissions at the relay nodes are triggered by using hardware ACKs. To further increase packet reception probability, channel diversity is exploited using a predefined hopping sequence. Protocol performance is experimentally evaluated by implementing it using CT-friendly IEEE 802.15.4 radio transceivers.

6.1 INTRODUCTION

The exploitation of CT in WSNs has already been demonstrated, for instance in Glossy [26], Splash [15], Sparkle [62] and Disco [53]. However, CT only work (packet is not broken and can be recovered) if the senders synchronize their transmissions with sub-microsecond precision. In these protocols, the synchronization is achieved by finely tuning the retransmissions, adjusting the software running in the main microcontroller at the instruction level. For example, with an IEEE 802.15.4 radio working at 2.4 GHz, the

maximum tolerable temporal displacement of concurrent packet transmissions is 0.5 μs [26].

To improve the synchronization, in RedFixHop the simultaneous packet transmissions at the relay nodes are triggered using the hardware ACKs of the radio transceiver; the microcontroller is thus bypassed. Hardware ACKs are transmissions triggered autonomously by the radio transceiver. To achieve this behavior with commercial components, transceivers with automatic ACK feature are used. Automatic ACKs are used to disseminate the packet, since they are normally generated after a deterministic and highly-accurate delay, following the reception of the last symbol of the previously received packet. Hardware ACKs are usually implemented in IEEE 802.15.4 radio transceivers [32] and controlled autonomously by the radio, without interference from the firmware running in the microcontroller. This avoids hard-to-predict firmware delays and jitter that occur in software-initiated transmissions. With a great stability and robustness against hardware and firmware variabilities, RedFixHop's CT work in an extremely reliable and scalable way.

Using an ACK-based flooding mechanism, instead of dynamic routing, allows the transmission of data packets with optimal latency and minimum complexity, since no previous knowledge of the network state is required and no communication overhead is introduced for route discovery. Combining flooding with a synchronous radio duty-cycling mechanism based on periodic active bursts, as shown in Fig. 6.1, energy consumption is also optimized [17] [47].

As the ACKs are used for flooding, the message reception confirmation service is lost. Instead, to increase reliability, packet retransmissions based on time redundancy and frequency diversity (multiple packet repetitions in different channels) are exploited. Since the wireless channel properties are time- and frequency-dependent, retransmissions on different channels increase the reception probability [55]. However, diversity is also problematic, because energy consumption is increased with redundant retransmissions. The required degree of redundancy (repetitions and channels) must be estimated for a given scenario, based on prob-

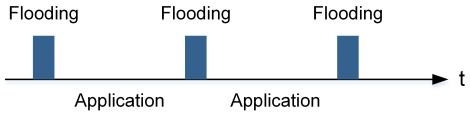

Figure 6.1: Synchronous radio duty-cycling mechanism (RedFixHop)

abilistic channel models, the network topology and the results of experimental tests.

6.2 REDFIXHOP PROTOCOL

This protocol exploits CT-based flooding with simultaneous transmissions triggered by hardware ACKs. To increase redundancy and diversity, every packet is repeated a fixed number of times. *RedFixHop* name is derived from this spatial redundancy and fixed repetition scheme.

The flooding uses synchronous radio duty-cycling based on periodic active bursts (Fig. 6.1). Only one source-to-sink message is transmitted in each burst. Between the flooding bursts, the radio of the nodes can be kept off to save power. The time between flooding slots is application-dependent, taking into consideration the existing trade off between latency and energy consumption [47]. The length of the burst (number of repetitions) is measured to provide a high probability of packet reception in the sink, based on its distance from the source (needed hops) and the interference level (packet losses). The burst mechanism is repeated a fixed number of times and with a predefined number of software-initiated hops.

At first, we assume that only one hardware ACK (one layer of relays) is enough to transmit the information from source to sink, as shown in Fig. 6.2. In this scenario, the proposed flooding mechanism works as follows (Fig. 6.3):

1. Every node is synchronized to turn its radio on at the beginning of the flooding period.

2. The transmission source sends the packet.

3. All the relays receiving the original packet from the source transmit it immediately, using hardware ACKs; potentially interfering constructively or exploiting the capture effect [56].

4. Repeat steps two and three until a predefined number of burst repetitions are reached. This is to increase reliability and ensure that all the potential receivers in the range of the source are synchronized and cooperating to generate the CT.

5. When the repetitions are over, the radios switch off until the beginning of the next flooding cycle.

Every node in the network gets synchronized after its first packet reception, since every transmitted packet contains enough information, the value of the counter field, to be located inside the burst period. After a number of bursts (depending on the clock drift of the microcontrollers) without receiving a packet, the node goes back to the unsynchronized state and keeps its radio on until a new packet is received.

As mentioned, the accurate time synchronization needed to achieve nearly-error-free CT is obtained using the automatically generated hardware ACKs from the radio transceivers. For example, IEEE 802.15.4 2.4 GHz radio transceivers implement the automatic sending of an ACK after 12 symbol periods following the end of the received frame [32]. This hacking or misuse of the ACKs creates an important drawback by limiting the maximum payload of the transmitted packets to 1 byte, including the $c + n$ bits allocated for the counter and hop fields. This is because the information must be encoded in the Data Sequence Number field of the MAC Header (Fig. 6.4). All other fields of the original packet are not copied in the ACK structure set by the IEEE 802.15.4 standard [32].

If multiple hops are required to reach the sink from the source, as shown in Fig. 6.5, the flooding mechanism is done by alternating rounds of hardwareACKs with rounds of software-initiated packet transmissions (software ACKs), requested immediately in the reception interrupt of the hardware ACKs (Fig. 6.6). This mech-

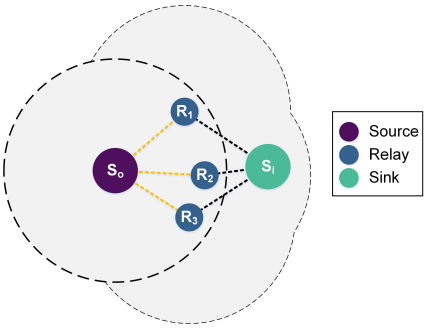

Figure 6.2: Source-to-sink communication with only one level of intermediate relays

anism is needed because the radio transceiver cannot be modified to automatically acknowledge a hardware ACK, since the ACK.Req bit is automatically cleared [32].

Using simultaneous hardware ACKs achieves higher synchronization accuracy than using software ACKs [18]. This is because we must take into account the jitter and delay, δ, introduced by the instructions executed in the microcontroller to trigger the transmission, as shown in Fig. 6.7 and Fig. 6.8.

A channel-hopping scheme, as shown in Fig. 6.9, is proposed to further increase reliability. Each counter repetition of the protocol (with or without software ACKs) is repeated on a predetermined sequence of channels, including a guard interval, t_{cs}, to account for the time required to perform the channel switching.

Adding frequency diversity by repeating the flooding on different channels, we increase the packet reception probability in the presence of frequency-dependent interference or jamming [55].

6.3 EXPERIMENTAL RESULTS

RedFixHop is implemented using TelosB motes, each of which has a TI CC2420 IEEE 802.15.4 radio transceiver and a TI MSP430 microcontroller.

To evaluate the differences between hardware and software ACKs we use three motes: source, relay and sink. The time be-

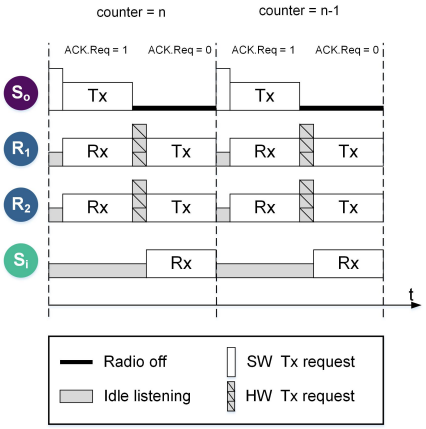

Figure 6.3: RedFixHop (Zero-SW-Hops)

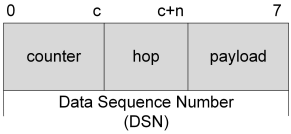

Figure 6.4: Payload codified in the Data Sequence Number field (IEEE 802.15.4)

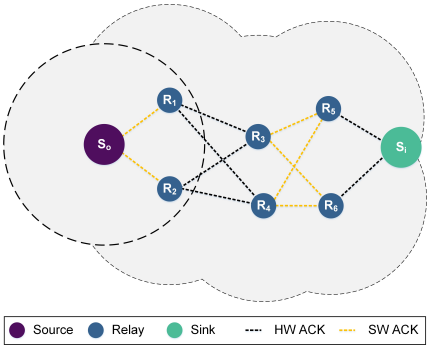

Figure 6.5: Source-to-sink communication with multiple levels of intermediate relays

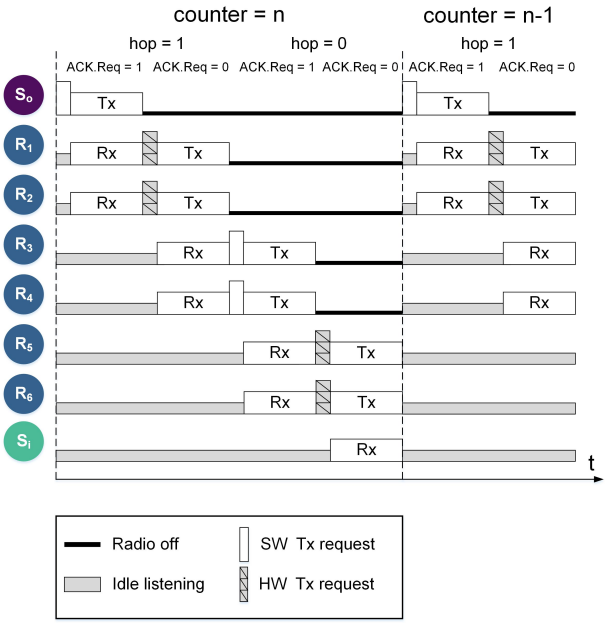

Figure 6.6: RedFixHop (Multi-SW-Hops)

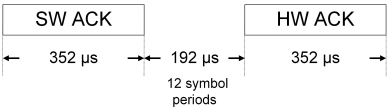

Figure 6.7: Hardware ACK timing

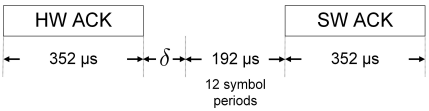

Figure 6.8: Software ACK timing

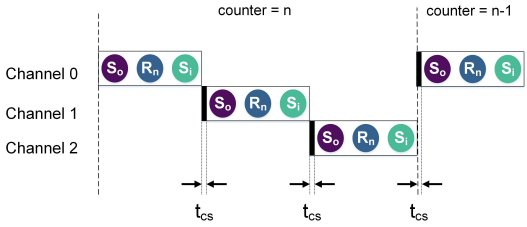

Figure 6.9: RedFixHop (Multi-Channel)

tween the end of the packet transmission from the source and the reception in the sink of the packet forwarded by the relay is measured (ACKs arrival time, t_{meas} in Fig. 6.10). After 1,000,000 tests, the results are shown in Table 6.1, and can be approximated using the normal distribution shown in Fig. 6.11, due to the central limit theorem [18].

The jitter, characterized by the standard deviation, is bigger with the software ACK mechanism, since it requires the participation of the main microcontroller to send the SPI commands to the radio transceiver to trigger the transmission [18]. Jitter has a great impact in the protocol reliability, since it degrades the CT mechanism in the presence of multiple simultaneous senders [54].

Compared to other CT-based flooding protocols, like Glossy (Fig. 6.12), which feature software-triggered transmissions, with RedFixHop and its hardware-triggered transmissions the maximum number of concurrent transmitters before the packet breaks is greatly increased.

Considering a chip period, T_C, of 0.5 μs in IEEE 802.15.4 with DSSS [32] [54], from Eq. 3.8:

$$N_{Software-ACK} \leqslant \left(\frac{T_C}{6\sigma_{SWACK}}\right)^2 = \left(\frac{0.5\mu s}{6 \times 167.3ns}\right)^2 \simeq 1\, Transmitters \tag{6.1}$$

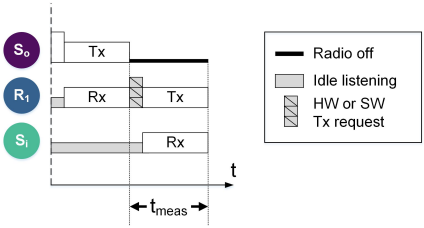

Figure 6.10: Experimental scenario to test SW and HW ACKs performances

$$N_{Hardware-ACK} \leq \left(\frac{T_C}{6\sigma_{HWACK}}\right)^2 = \left(\frac{0.5\mu s}{6 \times 22.5ns}\right)^2 \simeq 55\, Transmitters \tag{6.2}$$

The hardware ACK rounds are around 50 times more scalable than the software ACK rounds, which should break if there is not a single dominant transmitter. This is a worst-case result, since it neglects the DSSS coding gain and the capture effect due to the energy differences of the multiple transmissions when they arrive at the receiver. In practical scenarios, CT-based protocols also work with software-triggered retransmissions in TelosB motes, as we will see in the next chapter (BigBangBus); but it shows how scalability is roughly increased between ten to fifty times (depending on the synchronization quality, or jitter, σ, of the particular software implementation) with respect to state-of-the-art protocols (from tenths to hundreds of concurrent transmitters [36]), validating the expected outcome. Furthermore, number of transmissions per node are decreased, since every node is sent to sleep after transmitting, dramatically decreasing power consumption (Fig. 6.5). The biggest drawback is the lost of flexibility in the packet structure and the limited payload, which are the reasons why in the next chapter we introduce BigBangBus, a CT-based protocol working exclusively with flexible software-triggered retransmissions.

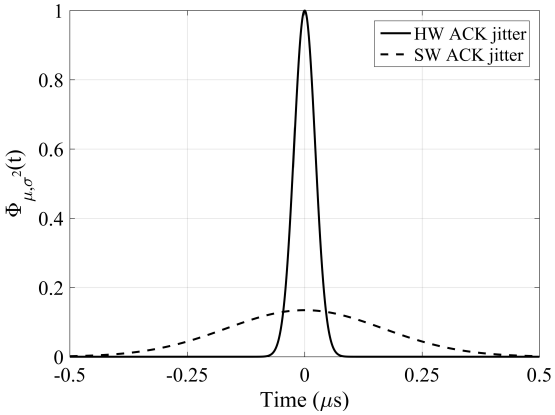

Figure 6.11: PDF of the ACKs arrival time normalized to zero mean

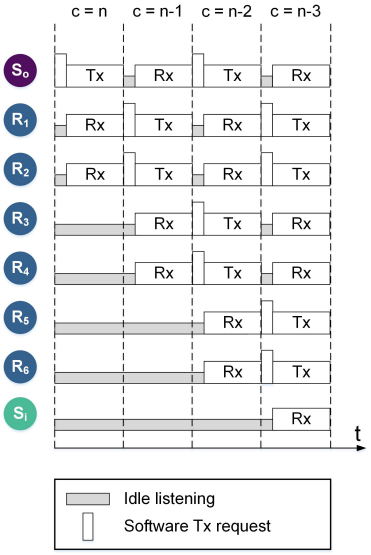

Figure 6.12: Classical Glossy mechanism

	Mean (μs)	Standard deviation (ns)
Hardware ACK	545,5	22,5
Software ACK	798,6	167,3

Table 6.1: ACKs arrival time

6.4 CONCLUSIONS

Exploiting hardware ACKs, very small packets of up to eight bits using commodity IEEE 802.15.4 radio transceivers can be disseminated in a WSN with optimal latency and high reliability, in a one-to-all or source-to-sink scenario.

RedFixHop's effectiveness was proven at the Dependability Competition of the EWSN, when it took First Place in 2016 [36] and Second Place in 2017 [20]. It also won Best Demo at the IEEE International Conference on Sensing, Communication and Networking (IEEE SECON 2016) [21].

In the future, to overcome the payload length and software ACKs limitations, the protocol can be implemented using radios with a programmable MAC unit [43], wireless microcontrollers, flexible FPGAs, or SDRs. In these flexible components, the behavior can normally be tweaked to allow the coding of longer payloads, the generation of several rounds of hardware ACKs without alternating them with poorly synchronized software ACKs, and the inclusion of native channel hopping and security (authenticated encryption) features. Modern wireless microcontrollers (like the Nordic nRF52 family) already provide flexible peripherals to automatically trigger retransmissions (of packets of arbitrary payload) without the intervention of the application microcontroller, avoiding variable delays due to a different number of executed instructions in different relay nodes.

With no routing overhead, RedFixHop achieves optimal latency and reliability, even during dynamic and harsh conditions. Unconventional use of commodity IEEE 802.15.4 hardware is shown

to obtain hardware-triggered CT-based flooding, hacking the ACK behavior.

To summarize, we demonstrate that flooding protocols based on CT are a promising, reliable and simple solution for self-healing multi-hop networks working in harsh environments, particularly for modulations with CT-friendly channel coding, like the DSSS used in IEEE 802.15.4 [57].

7

BIGBANGBUS: DECENTRALIZED ULTRA-LOW LATENCY NETWORK FLOODING

BigBangBus [23], a wireless bus based on flooding, CT, and the capture effect, is proposed to achieve highly reliable broadcast communication in a WSN working in harsh environments. It is designed to work in multi-source-to-multi-sink topologies, where multiple hops are required (Fig. 7.2). Different sources access the medium without colliding using network-wide predefined time slots and frequency channels. Frequency-, spatial- and time-diversity are exploited using redundant retransmissions. With self-healing characteristics, after the network is started (BigBang), it runs in a robust and decentralized way, with no master nodes in charge of the synchronization. Precise guard times are generated without using the fast (and usually inaccurate) microcontroller clock introducing long preambles between successive transmissions.

7.1 INTRODUCTION

CT only work if the senders synchronize their packet transmissions with sub-microsecond accuracy (0.5 μs with an IEEE 802.15.4 radio working at 2.4 GHz [26]). In RedFixHop (Chapter 6), the required synchronization precision is achieved using hardware-triggered retransmissions (misusing the automatic ACK feature), instead of conventional software-triggered packet transmissions. However, commercial radio transceivers limit the efficacy of this mechanism, restricting the payload and structure of the packets [19].

To overcome this limitation, BigBangBus, a protocol using flexible software-triggered retransmissions, is proposed. The resulting synchronization accuracy is worse than in RedFixHop and its hardware ACKs, but a number of considerations make it worth it:

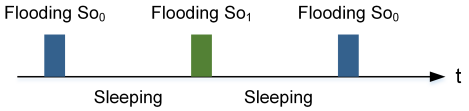

Figure 7.1: Synchronous radio duty-cycling mechanism (BigBangBus)

A. Thanks to the combination of the capture effect with modulations featuring CT-friendly channel coding, like the DSSS used in IEEE 802.15.4, the performance is not dramatically affected by the worse synchronization accuracy of software-triggered transmissions [56]. This is demonstrated in protocols like Glossy [26], Splash [15], Sparkle [62] and Disco [53].

B. To improve reliability in noisy environments, it is possible to switch to a different channel between packet retransmissions, as shown in Fig. 7.3. This is normally not possible using hardware ACKs, since the radio transceiver forces the transmission to take place in the same channel as the one used for reception.

C. The packet structure and length of the payload can be freely chosen, removing the stringent limitation of 1 byte of the IEEE 802.15.4 standard ACKs [32]. Short packets (up to a few bytes) are still preferred to decrease the resultant clock drift, since BigBangBus sends several packet repetitions without performing a resynchronization (Fig. 7.3).

7.2 BIGBANGBUS PROTOCOL

BigBangBus is based on scheduled flooding bursts (Fig. 7.1), each initiated by a predefined source. It works as follows (Fig. 7.3):

1. Every node is synchronized to turn its radio on at the beginning of the flooding period.

2. The source assigned to this period sends the packet, with several repetitions, in a predefined channel sequence.

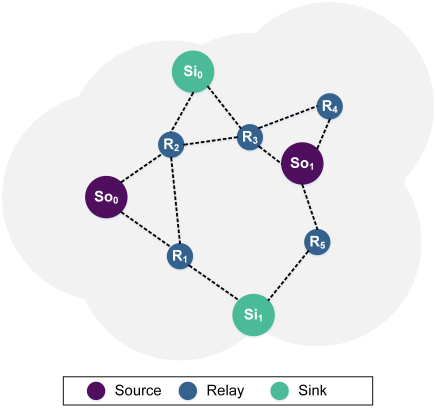

Figure 7.2: Multi-source-to-multi-sink communication with multiple levels of intermediate relays

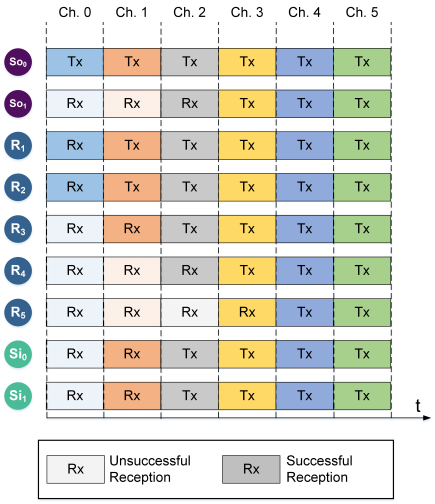

Figure 7.3: Flooding period of So_0

3. All the relays receiving the packet transmit it immediately, following the same channel sequence, potentially exploiting the capture effect.

4. When the flooding period has finished, the radios switch off until the beginning of the next flooding cycle.

In BigBangBus, the time slots are predefined, with no central authority in charge of the scheduling, making it extremely robust due to its decentralized nature. It can survive situations in which sources cannot listen each other during a certain amount of time without stopping the bus activity.

The initialization of the bus (BigBang phase), with the goal of achieving a network-wide consensus, is performed using the following protocol:

1. Every node that joins the bus listens for a few (random) cycles.

2. If a transmission is detected, the node joins the bus and learns when to start its slot in the flooding period (in case it is a source). If a transmission is not detected, the node initializes a new instance of the bus, arbitrarily setting the temporal starting point of its slot, and autonomously maintains this schedule, even if it is the only source in the bus at the moment. This mechanism is done only once in the lifetime of the network (or until the node is restarted).

3. Every time a packet is received, the node readjusts its synchronization, based on the information about the flooding period contained in the packet (packet source and counter value), eliminating accumulated temporal errors in every successful reception, and leading to a consensus in the network timing, in case different unstable schedules are generated during the start-up phase. The schedule is expected to converge, after start-up, in a few cycles.

In Fig. 7.4, we can see an example of BigBangBus working with the following configuration:

A. Four source nodes, sending six packet repetitions each, in three different channels.

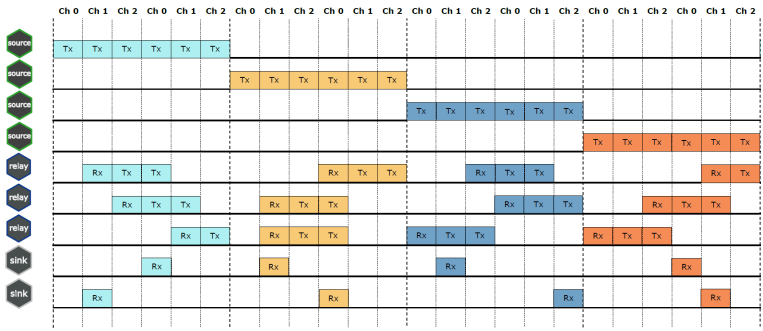

Figure 7.4: Example of a possible BigBangBus network-scheduling

B. Relays sending two packet repetitions after a successful reception.

The end-to-end latency experienced by each source of the network, given no gap is inserted between their slots, is bounded:

$$Latency_{average} \simeq \frac{t_{packet} \times R \times S}{2} \tag{7.1}$$

$$Latency_{maximum} \simeq t_{packet} \times R \times S \tag{7.2}$$

Being $t_{packet}$the time length of the packet, R the number of repetitions sent by each source and S the number of sources in the bus.

7.3 LOW-LEVEL OPTIMIZATIONS

BigBangBus is implemented using TelosB motes, each of which has a TI CC2420 IEEE 802.15.4 radio transceiver and a TI MSP430 microcontroller. This combination is purposely challenging, since it features little memory and timing resources. Therefore, extensive low-level optimizations are needed. Microcontroller and radio registers are directly accessed and fine-tuned to achieve optimal performance. Assembly language is needed in critical parts, like synchronization timers.

BigBangBus's distinctive features are:

A. *Sub-microsecond high-resolution timers*. Since retransmissions triggered by software are employed, accurate timers are needed in the microcontroller to reliably exploit the capture effect. Timers are calibrated with an algorithm that combines the fast and inaccurate, RC-type oscillator with the slow, accurate, 32 kHz crystal oscillator, the latter used as reference. With the TI MSP430 microcontroller used to test the protocol, with an internal Digitally Controlled Oscillator (DCO) of approximately 5 MHz (with strong variability between different nodes), sub-microsecond accuracy is achieved. Recalibration is periodically performed during run-time, since DCO operating frequency strongly depends on variable factors like temperature and operating voltage.

B. *CT-suitable modulation and channel coding*. Success of CT and the capture effect is dramatically affected by the low-level behavior of the demodulator. DSSS used in 2.4 GHz IEEE 802.15.4 is a key factor [38]. OQPSK with half-sine chip shaping is a non-linear modulation; it can be seen as equivalent to a MSK modulation [46], a form of Continuous-Phase Frequency-Shift Keying (CPFSK); which in constrast to pure **PSK!** (PSK!) modulations, also features FSK properties, better equipped to deal with CT, as seen in Chapter 5. In addition, using longer preamble and Start Frame Delimiter (SFD) fields generally leads to increased chances of reducing false frames detected due to noise.

C. *Optimal packet structure with extensive Cyclic Redundancy Check (CRC) coverage*. BigBangBus is designed for scenarios where an extremely high level of interference is expected. In these unusual and particularly harsh environments, reliable error detection is a challenging task. BigBangBus uses CRC techniques with polynomial sizes similar to the size of the payload, leading to extremely low chances of undetected errors in the packet. Optimal lossless payload compression techniques are also exploited.

D. *Power randomization and pseudo-random channel-hopping*. Wireless channel is expected to change quickly, with interference randomly hopping between channels. With pseudo-random sequences, a higher level of diversity is introduced, since channels are used in a different order in every repetition of the flooding sequence. In addition, introducing some degree of randomization in the transmission power of the nodes, generally decreases collisions due to a high number of concurrent transmitters, improving scalability.

E. *High-priority flows and smart slot skipping*. Different priorities are assigned to the sources, with those of higher priority being scheduled more often in the flooding burst, achieving lower latency. Furthermore, to save energy, relays can decide whether to send in every slot of the sequence or to sleep in some of them, based on measured parameters, such as Received Signal Strength Indicator (RSSI), Link Quality Indicator (LQI) and the number of unsuccessful receptions.

7.4 LONGER PREAMBLES

The internal DCO of the MSP430 is inaccurate, requiring complex calibration mechanisms if a time resolution higher than the one provided by the precise 32 kHz external crystal oscillator is needed. The time step of the 32 kHz oscillator (30.5 μs) is similar to the time required to send a byte (32 μs). It is challenging to implement a flooding scheme with guard times spanning a few byte periods, while keeping the tight synchronization required for CT to work (around 0.5 μs [26]).

RedFixHop was designed for extremely short packets (1 Byte payload), so packet losses and collisions due to synchronization errors were not so costly. Longer packets force the implementation of better synchronization techniques, since time- and energy-costs of packet retransmissions are high.

In order to keep the complexity low, flooding and channel-hopping synchronization mechanisms only use the slow 32 kHz oscillator. As a novelty, guard times between packet transmissions are generated using the accurate radio transceiver clock, by

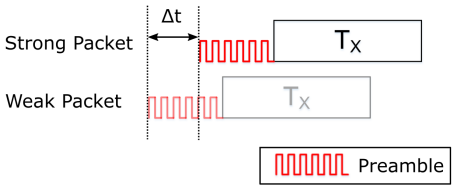

Figure 7.5: Capture effect is triggered if $\Delta t <$ (Preamble Duration)

increasing the length of the preamble [25]. Since receivers do not need to detect the whole preamble to synchronize, repetitions can be continuously triggered without calculating inaccurate delays with the microcontroller clock.

An additional positive effect of using longer preambles is the enhancement of the capture effect. Since radio transceivers do not effectively start the packet reception until the SFD is detected, longer preambles favor the synchronization with the most energetic reception, considering that the preamble is long enough so that simultaneous transmissions arrive with a relative delay lower than the total duration of the preamble. The capture effect applies, and packets can be received with high probability, even when the strongest transmission arrives later (Fig. 7.5), as long as it arrives before the reception of the previous preamble finishes .

The preamble is extended from the IEEE 802.15.4 standard specification, 4 Bytes (128 μs), to 10 Bytes (320 μs); adding an accurate guard time of 192μs (more than 6 ticks of the 32 kHz oscillator). The cost of improving the synchronization robustness is the additional time and energy spent in every transmission, but it greatly pays off due to the decreased number of packet losses and collisions.

7.5 CONCLUSIONS

BigBangBus's effectiveness was proven at the Dependability Competition of the EWSN, when it took First Place in 2018 [23], demonstrating the applicability of CT-based protocols in complex scenarios, combining different traffic patterns (point-to-multipoint and

multipoint-to-point) with a very high level of interference. Packets with small payloads, of just a few bytes, and real-time multihop communication scenarios, where packet reception acknowledgments are impractical, are optimal for BigBangBus, since the cost of redundant retransmissions is compensated by the impressive results in terms of latency and reliability.

In general, CT can outperform routing-based schemes thanks to their simplicity; opening a promising alternative in the, traditionally complex, field of mesh networking, particularly for real-time traffic and extremely noisy environments.

Part IV

CONCLUSIONS

8

CONCLUSIONS AND FUTURE WORK

In Part ii and Part iii, we established a theoretical and empirical background, introducing the required tools and results to understand CT in several levels:

A. *Analytical*. For the simple baseband case, with ideal rectangular pulses, an exact solution for the BER when two concurrent transmitters overlap is obtained (Eq. 3.1). It is used as the base upon the rest of the discussion is built. It provides a first important insight: keeping the time displacement lower than the sample period is key for any practical (low BER) use case. It also explains and predicts the peaks on the BER that appear at temporal displacement multiples of the sample period.

B. *Simulations*. Adding more elements to the system, like pulse shaping and the beating effect, makes it complex to find an analytical closed-form expression. A more effective approach is performing efficient baseband-equivalent simulations to predict the performance. Adjustments in the baseband model to include the impact of beating are introduced (Appendix A), and the capture area is obtained for different modulation schemes. The main result is that, while amplitude and phase distortions can be challenging for coherent-receivers, simple non-coherent receivers and frequency modulations work efficiently in combination with CT.

C. *Testbeds*. Finally, the expected results are validated in real-work protocols, implemented in commodity hardware, and obtaining promising results in terms of latency, simplicity and reliability.

Concurrent transmitters are fundamentally non-coherent. They do not hold a fixed phase relationship, and do not even have exactly the same carrier frequency. A visual analogy can be made

with light bulbs. While they are non-coherent sources, the more bulbs we turn on, the brighter (in average) it gets. If we slowly begin to modulate the light bulbs (with an OOK scheme), and we assume they are fast enough, a light detector can decode this bitstream, given that the bulbs are well synchronized. As we increase the number of bulbs, the energy transmitted increases and the signal becomes extremely hard to interference by external agents (like ambient noise). The main source of losses is then the internal interference due to synchronization errors between the bulbs, which can be easily controlled by limiting the sampling frequency, and the amplitude modulation caused by the beating effect. This analogy can be extended to frequency modulations, if we think of a scheme in which we use different light colors for the different symbols. While the performance is not the same as a single source of light sending with combined energy, the topology is very simple, robust, and particularly hard to disturb or jam.

In Section 8.1, we summarize the results of CT-based protocols performance for different modulation schemes, stressing the impact of the receiver low-level architecture. In Section 8.2, we discuss the practicalities of implementing real protocols using CT, and the impact of the digital clock frequency. Then, we discuss with more detail the applicability of CT in 2.4 GHz IEEE 802.15.4 and BLE (Section 8.3) . After that, we discuss briefly about the energy efficiency of CT (Section 8.4). Finally, in Section 8.5, we discuss future opportunities enabled by CT-based protocols and CT-friendly communication systems.

8.1 OVERVIEW OF CONCURRENT TRANSMISSIONS PERFORMANCE

CT protocols perfectly match simple, low-cost and low-power non-coherent receivers, as those typically used in IoT devices to demodulate BLE or IEEE 802.15.4 transmissions. It is generally thought that coherent receivers perform better than their non-coherent counterpart, and they do in typical AWGN channels. But this is not always the case. CT, and other effects, such as frequency selective fading due to phenomenons like multipath, make non-coherent

receivers superior in multiple practical environments, in addition to their inherent advantages in terms of complexity, cost and power consumption. This is particularly true for the relatively low data-rate links (up to 2Mbps) typically used in a low-power WSN. CT-based protocols are not a wise option for multimedia and power-hungry applications (where WiFi is typically used), with complex high-rate coherent modulations (like Quadrature Amplitude Modulation (QAM)) [28]; but CT are perfectly suitable for simple IoT applications, when latency and reliability need to be optimized, particularly in dense mesh networks and harsh scenarios, like industrial environments.

One consequence of using CT is that the network, if tightly synchronized, becomes immune to external noise and jamming:

$$if\ N_{max} \gg 2; \quad then\ BER \to 0 \quad when\ N \to N_{max} \tag{8.1}$$

Given that the energy of the N combined transmissions is much higher than the noise level, N_0 :

$$NE_b \gg N_0 \tag{8.2}$$

This is applicable to communication systems in which the error inside the capture area is zero, the catch being the energy cost of all the simultaneous transmissions.

CT is a reliable tool to deploy dependable IoT mesh networks in extremely noisy and demanding scenarios. The error is mainly fixed by the internal network interference, and the performance is defined by the ability of the transceivers to survive the beating and to keep the tight synchronization. The impact of external factors is minimized.

In Table 8.1 an overview of result for different communications systems is presented. The BER column specifies the maximum error encountered inside the capture area (defined for two concurrent transmitters and without noise); only those with zero error are scalable and have a practical interest.

MODULATION	CAPTURE AREA	BER	SCALABLE?
Baseband	Fig. 5.12	$BER \simeq 0$	Yes, Eq. 5.16
Baseband with Pulse Shaping	Fig. 5.13	$BER \simeq 0$	Yes, Eq. 5.16
Coherent BPSK	Fig. 5.14	$BER \leq 0.5$	No
Non-Coherent BFSK	Fig. 5.15	$BER \simeq 0$	Yes, Eq. 5.16

Table 8.1: Overview of CT performance for different communication systems

8.2 IMPLEMENTATION OF CONCURRENT TRANSMISSION PROTOCOLS IN DIGITAL SYSTEMS

Real protocols are constrained by the limited clock accuracy of wireless transceivers and application microcontrollers. Usually, CT-based protocols, such as BigBangBus (Chapter 7), achieve synchronization at the instruction level. It means that these protocols force the number of executed instructions after a packet is received to be the same in every concurrent transmitter. The lowest achievable temporal displacement is, then, roughly determined by the clock frequency (assuming instructions of one clock cycle).

With the 68-95-99.7 rule for normal distributions, we can approximate the temporal standard deviation, for software-triggered retransmissions, as:

$$\sigma \simeq \frac{1}{2f_{clock}} \tag{8.3}$$

Which means that 95% of the retransmissions are executed within a ± 1 instruction difference.

Combining this result with the Eq. 5.16, we obtain (Fig. 8.1):

$$N_{max} = \left(\frac{T_S f_{clock}}{3} \right)^2 \tag{8.4}$$

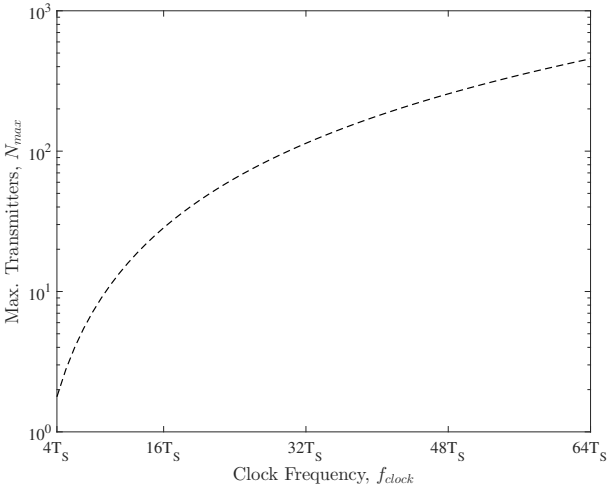

Figure 8.1: Maximum number of concurrent transmitters depending on the microcontroller clock frequency

Modern wireless microcontrollers for IoT tend to integrate in the same chip the application core and the wireless transceiver, decreasing synchronization inaccuracies due to the existing bottleneck in multi-chip solutions, that traditionally communicate using protocols such as SPI. Furthermore, many of them feature configurable peripherals and independent network co-processors, able to provide flexible automatic retransmissions support without having to explicitly command them with software instructions, greatly simplifying the application design.

Two of the most widely used protocols for low-power IoT devices are good matches for CT-based protocols: 802.15.4 at 2.4 GHz and BLE, as we discuss in the following section.

8.3 CONCURRENT TRANSMISSIONS IN IEEE 802.15.4 AND BLE

The 2.4 GHz physical layer of IEEE 802.15.4 is a standard for low power wireless networks used in a variety of protocols, like Zigbee, Thread and 6LoWPAN. The modulation used is OQPSK

with half-sine pulse shaping in combination with DSSS and soft-decision decoding. As we empirically demonstrated in Part iii, IEEE 802.15.4 radio transceivers are able to survive the interference of CT and effectively decode the packets. It seems to contradict our results, since OQPSK normally requires coherent phase demodulators, but the applicability of CT can be justified using two different arguments:

A. OQPSK with half-sine pulse shaping is equivalent to MSK, and thus can be non-coherently detected with a simple FSK demodulator tuned to a modulation index of 0.5 [66]. The coherent OQPSK demodulator has an excellent BER performance, but a complex design. In order to save cost, size, and particularly energy consumption, most IoT radios recover the modulated bitstream performing simple, non-coherent MSK demodulation. Non-coherent frequency demodulators are able to effectively cope with CT, as explained in Chapter 5. Furthermore, with the current trend of creating multi-protocol radio transceivers, the same demodulator can be used to non-coherently receive other FSK transmissions, like BLE.

B. DSSS is also used, together with soft-decision decoding, to increase the robustness of the transmission. It lowers the effective bitrate from 2 Mbps to 250 kbps. As a side effect, it eases the synchronization requirements of the CT, since the effective bit period is increased from 0.5 μs to 4 μs. Therefore, the chip sequences help to revert the distortion caused by the beating effect [38].

For BLE, the reasoning is similar. BLE uses Gaussian Frequency-Shift Keying (GFSK) with a BT product of 0.5 and a modulation index of roughly 0.5, what becomes close to the MSK used in IEEE 802.15.4. Therefore, similar non-coherent FSK demodulators, able to cope with CT, are used in typical low power radio radio transceivers in IoT applications. In the uncoded, fast data rate modes (1 Mbps and 2 Mbps) of Bluetooth 5 [12], the synchronization requirements are more demanding than in IEEE 802.15.4, since we lose the DSSS gain. However, in the coded, long range,

low data rate modes (500 kbps and 125 kbps) the requirements are not so demanding, since the effective bit period is increased (to 2 μ and 8 μ respectively).

In addition, the Bluetooth mesh networking protocol uses flooding as a simple and robust mechanism to build mesh networks. However, it is used in an asynchronous way, in which relays randomly send several unsynchronized repetitions in different advertising channels at random temporal offsets. This approach is different from the one proposed in our CT-based mechanism. In Bluetooth mesh, collisions are avoided by minimizing the number of retransmissions and randomizing the time slots and channels used by the relays. On the other hand, in CT-based protocols (RedFixHop and BigBangBus), destructive collisions are avoided by sending the repetitions in a tightly synchronized way. Anyway, the arrival of new protocols based on flooding further validates our approach, since it begins to appear as a real alternative to classical routing approaches.

8.4 ENERGY EFFICIENCY OF CONCURRENT TRANSMISSIONS

For the simple case that we use as reference (only two concurrent transmitters) the envelope of the resultant waveform is a sinusoidal (Fig. 8.2), so it can be easily analyzed by considering that the received energy has a sinusoidal shape [44]. However, when more than two concurrent transmitters with slightly different frequencies overlap, the sinusoidal approximation is no longer valid, and the envelope can take more complex shapes (Fig. 8.3 and Fig. 8.4).

In general, we can make the following remarks:

A. When all the concurrent transmissions overlap perfectly in phase, there is a temporal instant of pure constructive interference, in which the transmission achieves a very energetic peak. If we consider all the N individual transmitters arriving at the receiver with the same energy, E_b:

$$E_{b\,Constructive\ Interference}(N\ Transmitters) = N^2 E_b \gg N E_b \tag{8.5}$$

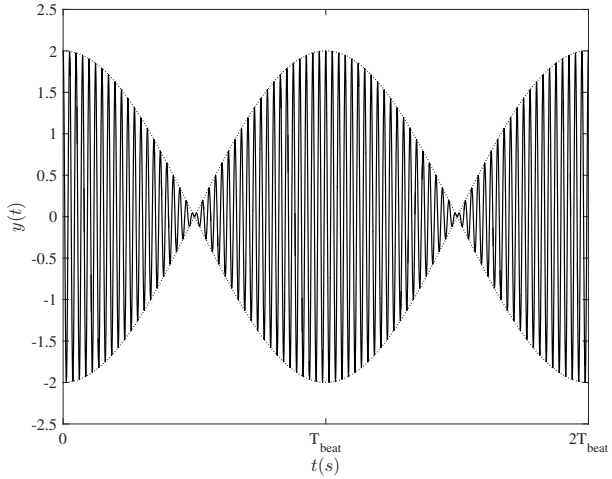

Figure 8.2: Received waveform with the overlap of two concurrent carriers with the same energy and slightly different frequencies: sinusoidal envelope

During this period, the energy is much stronger than the energy we would receive by sending with only one transmitter with N times the energy (NEb). This is an interesting result, since we can achieve short periods of energy higher than the sum of the energies we are sending, what can be used in very harsh scenarios to create very energetic bursts.

B. When all the transmissions overlap in purely destructive interference, the transmission completely fades (if all received with the same energy):

$$E_{b\,Destructive\,Interference}(N\ Transmitters) = 0 \tag{8.6}$$

C. In average, the energy is conserved:

$$Mean[E_b(N\ Transmitters)] = NE_b \tag{8.7}$$

Since the phase relationship between the independent local oscillators of the concurrent transmitters cannot be controlled, during a packet reception one can expect a quick succession of high

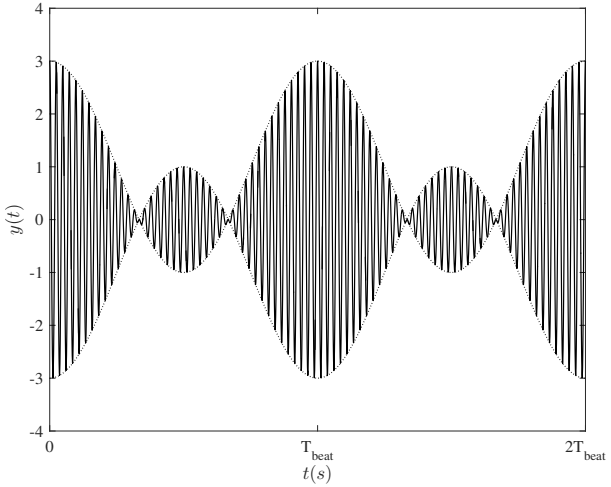

Figure 8.3: Received waveform with the overlap of three concurrent carriers with the same energy and slightly different frequencies: complex envelope

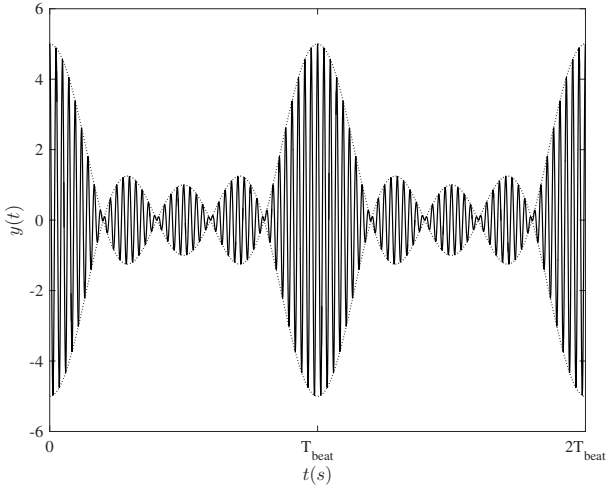

Figure 8.4: Received waveform with the overlap of five concurrent carriers with the same energy and slightly different frequencies: complex envelope

and low energetic periods. The length of these periods depends on the accuracy of the local oscillators. The higher the accuracy, and thus the lower the dissimilarity between their local frequencies, the longer the resultant beating period will be. Depending on the relationship between the symbol period and the frequency errors in the concurrent carriers, the beating period might be bigger than the symbol period. This is usually the situation with accurate crystals: the beating period spans the reception of multiple symbols.

A suitable modulation, and preferably the right channel equalization and codification techniques, are required to achieve an optimal CT performance and a good energy efficiency. Gain must be dynamically adjusted during the packet reception, since the received energy greatly fluctuates. There exists the potential to manage the highly energetic cycles, together with controlled beating periods, to design complex CT-oriented protocols that take into consideration the alternating periods of constructive and destructive interference when designing the physical layer, and choosing adequate symbol rates and crystal tolerances. Furthermore, introducing some degree of transmission energy randomization in the concurrent relays can be useful to trigger the appearance of dominant transmissions in some temporal intervals and favor the packet reception in particularly harsh areas by increasing the energy diversity.

Anyway, even when there is a lot of room for improvement if protocols are custom-made to cope with CT, we demonstrate the applicability CT-based flooding schemes in two physical layers of current IoT standards, BLE and IEEE 802.15.4, without requiring any further modifications. This fact demonstrates the simplicity and efficiency of the mechanism in low-power and low data rate FSK communication systems, without adding complexity and further packet processing that might result in an increased power consumption, size and cost of the IoT transceivers, what is normally not an option in the extremely competitive IoT ecosystem.

8.5 FUTURE WORK

CT constitutes itself as a promising mechanism to flood packets in harsh environments when latency and overhead need to be minimized, particularly for short packets that can be redundantly repeated without a big energy cost. Extremely robust protocols based on Time-Division Multiple Access (TDMA) with channel hopping (as BigBangBus) can be built upon the CT-flooding primitive, using existing inexpensive and simple IoT transceivers equipped with non-coherent FSK demodulators, such as those used for IEEE 802.15.4 and BLE. Current mesh protocols, like Bluetooth mesh networking, can be extended to use synchronized flooding, potentially improving their reliability, latency and scalability; enabling its usage in dependable IoT applications, such as those found in industrial environments.

There exists the potential to further analyze the effect with SDR systems, able to over-sample the received baseband in-phase and quadrature components, giving valuable insights about the distortion due to the CT. These measurements can be used to validate the analysis of Appendix A. Furthermore, while CT-based wireless mesh protocols also provide network-wide time synchronization by design [26], the usage of external common references, like GPS, can expand the possibilities to design more flexible protocols, with more accurate time and frequency adjustments.

The development of new radio transceivers and physical communication layers, built to effectively cope with CT is also a field of interest. They should feature a tight built-in retransmission synchronization mechanism, able to minimize the time misalignment between concurrent relaying nodes. Agile gain adjustment is also needed to cope with fluctuating received energy levels, due to the beating effect.

Moreover, security needs to be taken into consideration. A real-time and agile authenticated encryption/decryption mechanism, able to run in the tight time between successive packet repetitions, is needed in order to avoid the injection in the network of malicious packets that would be flooded and propagated. This potentially enables pernicious denial-of-service attacks to be performed at a low-energy cost [29][30][31].

Finally, as explained in Section 8.4, bit errors are not expected to be randomly and independently distributed, since they tend to appear in bursts during the valley periods of the combined waveform. The frequency of appearance of these valleys can be controlled using very accurate oscillators which, together with the bit period, can be tweaked to control the number of bit transmissions a valley spans. Similarly, the number of bits a peak spans can be adjusted. If the peak is wide enough, techniques like repeating the packets several times (as long as synchronization is not lost), so that one is received during an energy peak have interest for further research. In addition, burst error-correcting codes are a good match to recover the errors that may appear during valleys.

Part V

APPENDIX

A

BASEBAND-EQUIVALENT MODEL OF CONCURRENT TRANSMISSIONS

The following steps are proposed to characterize the applicability of CT in a given communication system:

1. Beginning with the baseband model, usually available in the literature for common systems, we make the required adjustments to work with over-sampled signals in order to perform simulations with a temporal resolution higher than the symbol period. This is important, since we want to characterize the effect of temporal displacements lower than the sampling period.

2. We model two concurrent transmitters, sending the same bitstream, and perform Monte Carlo simulations (with a large bitstream, to achieve stable values) for different relative energy levels (SIR) and relative time displacements (Δt), including the distortion introduced by the beating effect. Displaying the results in the region $-3\ dB \leq SIR \leq 3\ dB$ and $0 \leq \Delta t \leq 0.5 T_S$, the capture area is obtained

3. As a rule of thumb, the maximum error in the capture area is the error that we expect in a dense CT-based network using the characterized communication system. For CT to be of practical use, the capture area must be nearly error-free and the hardware and software used to deploy the network need to be precise enough to keep the equivalent temporal displacement of the N concurrent transmitters below half the symbol period ($\Delta t_{eq}(N) \leq T_S/2$).

In addition to the temporal displacement, the effect of the beating effect must be introduced in the signal received by the demodulator. This effect greatly varies depending on the working principle of the receiver. The model of the beating effect is presented for

coherent phase modulations (Section A.1) and for non-coherent frequency modulations (Section A.2).

A.1 CT-BASEBAND MODEL OF COHERENT PHASE MODULATIONS

For simplicity, we analyze the case of an antipodal coherent phase modulation with only two symbols (BPSK), but similar analyses can be performed for higher order constellations. The transmitted waveforms, $y_1(t)$ and $y_2(t)$, can be expressed as (neglecting the temporal displacement):

$$y_1(t) = A_1 \cos(2\pi f_{c1} t + \pi(1 - n(t))); \; n \in \{0, 1\} \tag{A.1}$$

$$y_2(t) = A_2 \cos(2\pi f_{c2} t + \pi(1 - n(t))); \; n \in \{0, 1\} \tag{A.2}$$

Assuming $A_1 > A_2$, and particularizing to one of the two possible transmitted bits ($n = 1$), the concurrent transmission, $y_{CT}(t)$, results (without considering ISI):

$$\begin{aligned} y_{CT}(t, n = 1) &= y_1(t, n = 1) + y_2(t, n = 1) \\ &= (A_1 - A_2) \cos(2\pi f_{c1} t) \\ &+ 2A_2 \cos\left(2\pi \frac{f_{c1} + f_{c2}}{2} t\right) \cos\left(2\pi \frac{f_{c1} - f_{c2}}{2} t\right) \end{aligned} \tag{A.3}$$

And its baseband equivalent can be modeled as:

$$y_{CT\ Baseband}(t, n = 1) \approx (A_1 - A_2) + 2A_2 cos(2\pi f_{beat} t) \tag{A.4}$$

$$f_{c1} \approx f_{c2} \approx f_c \tag{A.5}$$

$$f_{beat} = |f_{c1} - f_{c2}| \tag{A.6}$$

Assuming that the beating frequency, f_{beat}, has the following properties:

- The beating frequency is low enough so that it is not eliminated by the receiving-side matched filter. This is, the beating distortion is within the transmission bandwidth, what happens when the beating period, T_{beat}, is smaller than the symbol period, T_S:

$$T_{beat} = 1/f_{beat} \gg T_S \tag{A.7}$$

- The beating frequency is high enough so that a packet reception contains several beating periods:

$$T_{beat} \ll T_{packet} \tag{A.8}$$

These are realistic assumptions for practical scenarios and typical radio transceivers with usual frequency error tolerances. For example, in a standard IEEE 802.15.4 2.4 GHz transceiver with a crystal of $\pm 40\ ppm$, the expected beating frequency is in the kHz range:

$$f_{beat} \leq 192\ kHz \tag{A.9}$$

$$T_{beat} \geqslant 5.2\ \mu s \tag{A.10}$$

And, since OQPSK at 2 Mbps is used :

$$T_s = 1\ \mu s \ll T_{beat} \tag{A.11}$$

The effective bitrate (after the DSSS decoding) is 250 kbps, so a packet period, which spans the transmission of multiple bytes, is much longer than the beating period:

$$T_{packet} \gg T_{byte} = 32\ \mu s \gg T_{beat} \tag{A.12}$$

Going back to our analysis, after the signal is converted to its baseband equivalent, the bit decision takes place, using the following criteria in the comparator:

$$n = \begin{cases} 0 & y_{CT\ Baseband}(t, n = 1) < 0 \\ 1 & y_{CT\ Baseband}(t, n = 1) > 0 \end{cases} \tag{A.13}$$

What means that, even without external noise, the following condition must be satisfied:

$$A_1 > 3A_2 \tag{A.14}$$

Or, equivalently:

$$SIR > 10\,dB \tag{A.15}$$

In AWGN channels, a more conservative threshold was obtained in Section 4.3 ($SIR > 20\,dB$) to obtain the characteristic waterfall behavior of BER vsE_b/N_0 (Fig. 4.6).

In particular, when both concurrent transmitters are received with the same energy ($SIR = 0\,dB$), which is the condition we impose to enable scalable CT-based protocols, the decision is completely random, since the signal at the comparator swings around zero:

$$y_{CT\ Baseband}(t, n = 1, SIR = 0\,dB) = 2A_1 cos(2\pi f_{beat} t) \tag{A.16}$$

$$BER_{Coherent\ BPSK}(SIR = 0\,dB) = 0.5 \tag{A.17}$$

This is an analytical reasoning to discourage the usage of coherent phase demodulator with CT that agrees with the simulation results of Chapter 4. To further understand the effect of CT in the demodulator, the resultant constellation diagram after 1,000 random bit transmissions, including AWGN noise ($E_b/N_0 = 20\,dB$), for different SIR levels is displayed in Fig. A.1, Fig. A.2 and Fig. A.3. From $SIR < 10\,dB$, both symbols start to overlap and the error rate greatly increases, reaching 0.5 at 0 dB.

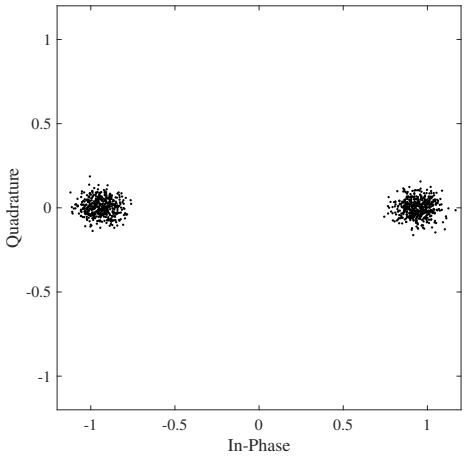

Figure A.1: Constellation for the reception of two concurrent transmissions with BPSK ($SIR = 30\,dB$, $E_b/N_0 = 20\,dB$)

Since the communication is only possible for $SIR > 10\,dB$ (preferably $SIR > 20\,dB$), the time displacement, Δt, is not particularly relevant in this scenario. To enable CT-based protocols, the receiver needs to dynamically detect the beating envelope zero crosses, and subsequently switch the decision sign for the zero and one symbols. This must be perform multiple times within a packet reception, what can be challenging without complex signal processing techniques and proper data encoding. Therefore, non-coherent frequency modulations constitute a much simpler choice.

A.2 CT-BASEBAND MODEL OF NON-COHERENT FREQUENCY MODULATIONS

For orthogonal BFSK signals, neglecting the temporal displacement and ISI, the waveforms can be expressed as:

$$y_1(t) = A_1 \cos(2\pi(f_{c1} + n(\Delta f_1))t);\ n \in \{-1, +1\} \qquad \text{(A.18)}$$

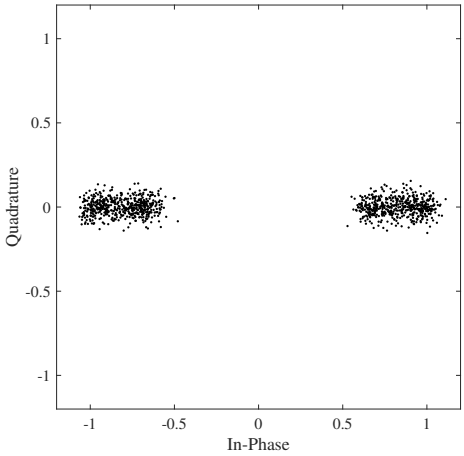

Figure A.2: Constellation for the reception of two concurrent transmissions with BPSK ($SIR = 20\,dB$, $E_b/N_0 = 20\,dB$)

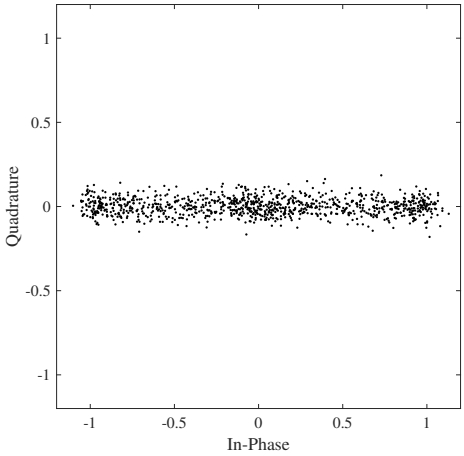

Figure A.3: Constellation for the reception of two concurrent transmissions with BPSK ($SIR = 10\,dB$, $E_b/N_0 = 20\,dB$)

$$y_2(t) = A_2 \cos(2\pi(f_{c2} + n(\Delta f_2))t);\ n \in \{-1, +1\} \tag{A.19}$$

$$f_{c1} \approx f_{c2} \approx f_c \tag{A.20}$$

$$\Delta f_1 \approx \Delta f_2 \approx \Delta f \tag{A.21}$$

For non-coherent demodulation, a simple envelope detector comparing the energy in the two orthogonal branches ($f_c + \Delta f$ and $f_c - \Delta f$) is used to model the demodulation process (Fig. 5.1). With two concurrent transmitters, the envelope detected in every frequency band fluctuates (considering $A_1 > A_2$):

$$Envelope(f_c + \Delta f) = \begin{cases} 0 & if\ n = -1 \\ (A_1 - A_2) + 2A_2 \left|\cos\left(2\pi \frac{f_{beat}}{2} t\right)\right| & if\ n = +1 \end{cases} \tag{A.22}$$

$$Envelope(f_c - \Delta f) = \begin{cases} (A_1 - A_2) + 2A_2 \left|\cos\left(2\pi \frac{f_{beat}}{2} t\right)\right| & if\ n = -1 \\ 0 & if\ n = +1 \end{cases} \tag{A.23}$$

Different waveforms and envelopes for different SIR levels are presented in Fig. A.4, Fig. A.5 and Fig. A.6. The average energy received in every branch of the comparator (assuming no noise, and an unit reference resistor) is:

$$Mean[Energy(f_c + \Delta f)] = \begin{cases} 0 & if\ n = -1 \\ (A_1 - A_2)^2 + \frac{(2A_2)^2}{2} & if\ n = +1 \end{cases}$$

(A.24)

$$Mean[Energy(f_c - \Delta f)] = \begin{cases} (A_1 - A_2)^2 + \frac{(2A_2)^2}{2} & if\ n = -1 \\ 0 & if\ n = +1 \end{cases} \tag{A.25}$$

In particular, when $SIR = 0dB$ ($A_1 = A_2$):

$$Mean[Energy(f_c + \Delta f, SIR = 0\,dB)] = \begin{cases} 0 & if\ n = -1 \\ 2(A_1)^2 & if\ n = +1 \end{cases} \tag{A.26}$$

$$Mean[Energy(f_c - \Delta f, SIR = 0\,dB)] = \begin{cases} 2(A_1)^2 & if\ n = -1 \\ 0 & if\ n = +1 \end{cases} \tag{A.27}$$

As a result, with simple non-coherent FSK detection, the system is expected to work even when $SIR = 0\,dB$, validating the simulations results of Chapter 5, and complying with the requirements to be of practical use in CT-based networks (zero error in the capture area).

The important insight is that the beating effect creates an energy fluctuation in the the branch of the transmitted bit, but it is not able to introduce energy in the orthogonal branch of the other bit. No bit inversions can be induced only by the beating effect itself, as opposed to the case with coherent BPSK demodulation, since the beating mainly distorts the amplitude and phase of the wave. In practical scenarios, a decreased noise resistant is observed during the destructive interference intervals. Temporal misalignments between the concurrent transmissions further affect the performance.

For only two concurrent transmitters and non-coherent BFSK, we can obtain the analytical expression of the expected BER, assuming that both transmissions are received with the same energy ($A_1 = A_2$):

$$E_b(t)_{BFSK}(A_1 = A_2) = 4E_{b0}\cos^2\left(2\pi\frac{f_{beat}}{2}t\right) \tag{A.28}$$

For simplicity, we consider no timing errors at the symbol level ($\Delta t = 0$) and a fairly constant energy during one bit reception ($T_{beat} \gg T_S$). Then, we can average the bit error rate during one beating period by using Eq. 5.10 together with the energy distortion created by the beating envelope:

$$\begin{aligned} BER_{CT\,BFSK} &= \frac{1}{T_{beat}}\int_0^{T_{beat}} \frac{1}{2}\exp\left(-\frac{E_b(t)}{2N_0}\right)\,\mathrm{d}t \qquad (A.29)\\ &= \frac{1}{2T_{beat}}\int_0^{T_{beat}} \exp\left(-\frac{2E_{b0}}{N_0}\cos^2\left(2\pi\frac{f_{beat}}{2}t\right)\right)\,\mathrm{d}t \\ &= \frac{\exp(-E_{b0}/N_0)}{2T_{beat}}\int_0^{T_{beat}} \exp\left(-\frac{E_{b0}}{N_0}\cos\left(2\pi f_{beat}t\right)\right)\,\mathrm{d}t \\ &= \frac{1}{2}\exp(-E_{b0}/N_0)\;\; \mathrm{I}_0\left(-E_{b0}/N_0\right) \end{aligned}$$

where $\mathrm{I_n}(z)$ is the modified Bessel function of the first kind.

The curve of Fig. A.7 is obtained, what perfectly agrees with the simulation results from Section 5.2 and Fig. 5.4. For more complex scenarios, with more than two transmitters, different relative power levels and temporal misalignments, finding an analytical expression results challenging, and probably even a closed-form expression for the energy envelope cannot be found. In these situations, simulation are more convenient and comparatively simpler to design.

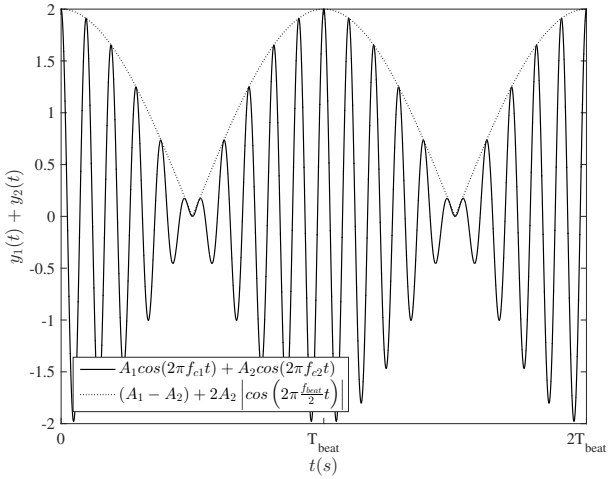

Figure A.4: Signal received with two concurrent transmitters of slightly different frequencies, including the envelope ($SIR = 0\ dB$)

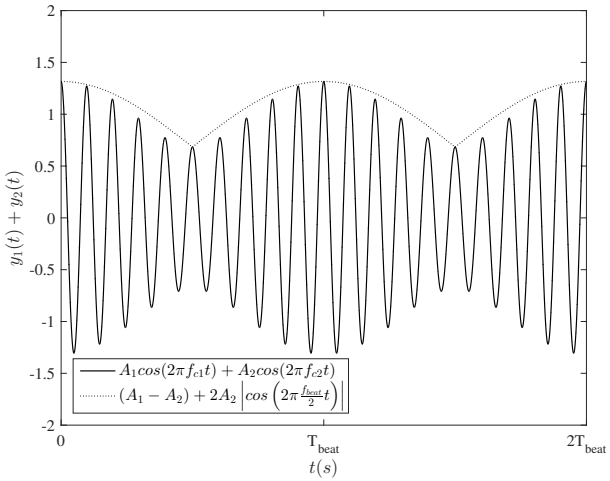

Figure A.5: Signal received with two concurrent transmitters of slightly different frequencies, including the envelope ($SIR = 10\ dB$)

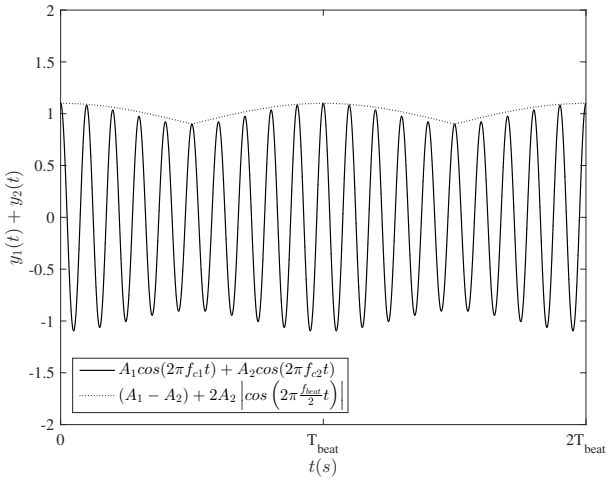

Figure A.6: Signal received with two concurrent transmitters of slightly different frequencies, including the envelope ($SIR = 20\ dB$)

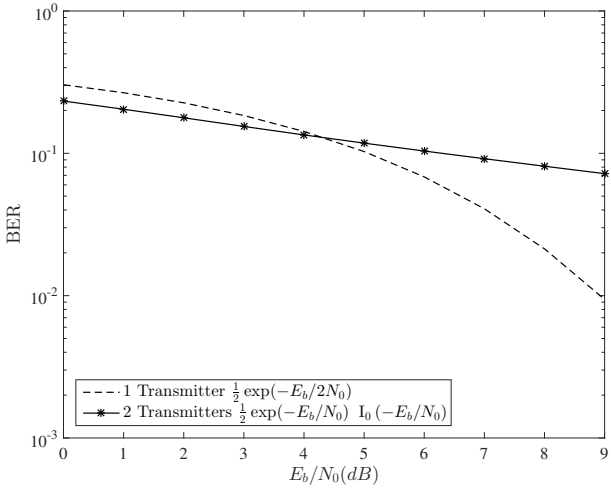

Figure A.7: Analytical BER for one transmitter and for two concurrent transmitters ($\Delta t = 0$ and $SIR = 0\ dB$) in non-coherently received BFSK

BIBLIOGRAPHY

[1] Ian F Akyildiz, Xudong Wang, and Weilin Wang. "Wireless mesh networks: a survey." In: *Computer networks* 47.4 (2005), pp. 445–487 (cit. on p. 9).

[2] Beshr Al Nahas, Duquennoy Simon, and Olaf Landsiedel. "Concurrent Transmissions for Multi-Hop Bluetooth 5." In: *EWSN*. 2019 (cit. on p. 12).

[3] Huda Alhalabi and Tat-Chee Wan. "Communication Protocol for Constructive Interference Flooding in Wireless Sensor Networks." In: *Journal of Theoretical & Applied Information Technology* 94.1 (2016) (cit. on p. 12).

[4] Huda AH Alhalabi, Tat-Chee Wan, Lial Missif, and Mohammed Ehalabi. "Performance analysis of the constructive interference flooding in wireless sensor networks." In: *Information Technology (ICIT), 2017 8th International Conference on*. IEEE. 2017, pp. 75–81 (cit. on p. 10).

[5] Mathias Baert, Jen Rossey, Adnan Shahid, and Jeroen Hoebeke. "The Bluetooth mesh standard: An overview and experimental evaluation." In: *Sensors* 18.8 (2018), p. 2409 (cit. on pp. 6, 14).

[6] Boris Bellalta. "IEEE 802.11 ax: High-efficiency WLANs." In: *IEEE Wireless Communications* 23.1 (2016), pp. 38–46 (cit. on p. 13).

[7] Kay Bierzynski, Antonio Escobar, and Matthias Eberl. "Cloud, fog and edge: Cooperation for the future?" In: *Fog and Mobile Edge Computing (FMEC), 2017 Second International Conference on*. IEEE. 2017, pp. 62–67 (cit. on p. 5).

[8] Martina Brachmann, Olaf Landsiedel, and Silvia Santini. "Keep the Beat: On-The-Fly Clock Offset Compensation for Synchronous Transmissions in Low-Power Networks." In: *Local Computer Networks (LCN), 2017 IEEE 42nd Conference on*. IEEE. 2017, pp. 303–311 (cit. on p. 60).

[9] Joseph Bradley, Joel Barbier, and Doug Handler. "Embracing the Internet of everything to capture your share of $14.4 trillion." In: *White Paper, Cisco* (2013) (cit. on p. 9).

[10] Marco Centenaro, Lorenzo Vangelista, Andrea Zanella, and Michele Zorzi. "Long-range communications in unlicensed bands: The rising stars in the IoT and smart city scenarios." In: *IEEE Wireless Communications* 23.5 (2016), pp. 60–67 (cit. on p. 9).

[11] Tengfei Chang, Thomas Watteyne, Xavier Vilajosana, and Pedro Henrique Gomes. "Constructive Interference in 802.15.4: A Tutorial." In: *IEEE Communications Surveys & Tutorials* (2018) (cit. on p. 12).

[12] Mario Collotta, Giovanni Pau, Timothy Talty, and Ozan K Tonguz. "Bluetooth 5: A concrete step forward toward the IoT." In: *IEEE Communications Magazine* 56.7 (2018), pp. 125–131 (cit. on p. 94).

[13] Pablo Corbalán and Gian Pietro Picco. "Concurrent Ranging in Ultra-wideband Radios: Experimental Evidence, Challenges, and Opportunities." In: *EWSN*. 2018, pp. 55–66 (cit. on p. 12).

[14] Fernando Moreno Cruz, Antonio Escobar Molero, Encarnacion Castillo, Markus Becherer, Almudena Rivadeneyra, and Diego P Morales. "Why Use RF Energy Harvesting in Smart Grids." In: *2018 IEEE 23rd International Workshop on Computer Aided Modeling and Design of Communication Links and Networks (CAMAD)*. IEEE. 2018, pp. 1–6 (cit. on p. 14).

[15] Manjunath Doddavenkatappa, Mun Choon Chan, and Ben Leong. "Splash: Fast Data Dissemination with Constructive Interference in Wireless Sensor Networks." In: *Presented as part of the 10th USENIX Symposium on Networked Systems Design and Implementation (NSDI 13)*. Lombard, IL: USENIX, 2013, pp. 269–282. URL: https://www.usenix.org/conference/nsdi13/technical-sessions/presentation/doddavenkatappa (cit. on pp. 65, 78).

[16] Robert Drosd, Leonid Minkin, and Alexander S Shapovalov. "Interference and the Law of Energy Conservation." In: *The Physics Teacher* 52.7 (2014), pp. 428–430 (cit. on p. 23).

[17] Adam Dunkels. "The ContikiMAC Radio Duty Cycling Protocol." In: *Swedish Institute of Computer Science* (2011) (cit. on p. 66).

[18] Prabal Dutta, Razvan Musaloiu-e, Ion Stoica, and Andreas Terzis. "Wireless ACK collisions not considered harmful." In: *Proceedings of the 7th ACM Workshop on Hot Topics in Networks (HotNets-VII)*. 2008, pp. 1–6 (cit. on pp. 69, 72).

[19] Antonio Escobar, Francisco J. Cruz, Javier Garcia-Jimenez, Jirka Klaue, and Angel Corona. "RedFixHop with channel hopping: Reliable ultra-low-latency network flooding." In: *2016 Conference on Design of Circuits and Integrated Systems (DCIS)*. Nov. 2016, pp. 1–4. DOI: 10.1109/DCIS.2016.7845367. URL: https://ieeexplore.ieee.org/document/7845367/ (cit. on pp. 12, 65, 77).

[20] Antonio Escobar, Javier Garcia-Jimenez, Francisco J. Cruz, Jirka Klaue, Angel Corona, and Divya Tati. "Competition: RedFixHop with Channel Hopping." In: *Proceedings of the 2017 International Conference on Embedded Wireless Systems and Networks*. EWSN '17. Uppsala, Sweden: Junction Publishing, 2017, pp. 264–265. URL: http://dl.acm.org/citation.cfm?id=3108009.3108073 (cit. on pp. 65, 75).

[21] Antonio Escobar, Cristian Gonzalez, Francisco J. Cruz, Javier Garcia-Jimenez, Jirka Klaue, and Angel Corona. "RedFixHop: Efficient Ultra-Low-Latency Network Flooding." In: *2016 13th Annual IEEE International Conference on Sensing, Communication, and Networking (SECON)*. June 2016, pp. 1–2. DOI: 10.1109/SAHCN.2016.7733012. URL: https://ieeexplore.ieee.org/document/7733012/ (cit. on pp. 65, 75).

[22] Antonio Escobar, Fernando Moreno, Antonio J Cabrera, Javier Garcia-Jimenez, Francisco J Cruz, Jirka Klaue, Angel Corona, Divya Tati, and Diego P Morales. "Demo: RedFixHop - Reliable Real-Time Network Flooding." In: *Proceedings of the*

2018 International Conference on Embedded Wireless Systems and Networks. Junction Publishing. 2018, pp. 197–198. URL: http://dl.acm.org/citation.cfm?id=3234885 (cit. on p. 65).

[23] Antonio Escobar et al. "Competition: BigBangBus." In: *Proceedings of the 2018 International Conference on Embedded Wireless Systems and Networks*. Junction Publishing. 2018, pp. 213–214. URL: http://dl.acm.org/citation.cfm?id=3234894 (cit. on pp. 6, 12, 77, 84).

[24] Antonio Escobar-Molero. "Improving reliability and latency of Wireless Sensor Networks using Concurrent Transmissions." In: *at - Automatisierungstechnik* 67.1 (Jan. 2019), pp. 42–50. DOI: 10.1515/auto-2018-0064 (cit. on pp. 3, 10, 11).

[25] Antonio Escobar-Molero, Javier Garcia-Jimenez, Jirka Klaue, Fernando Moreno-Cruz, Borja Saez, Francisco J Cruz, Unai Ruiz, and Angel Corona. "Competition: RedNodeBus, Stretching Out the Preamble." In: *Proceedings of the 2019 International Conference on Embedded Wireless Systems and Networks*. 2019 (cit. on pp. 6, 12, 84).

[26] F. Ferrari, M. Zimmerling, L. Thiele, and O. Saukh. "Efficient network flooding and time synchronization with Glossy." In: *Proceedings of the 10th ACM/IEEE International Conference on Information Processing in Sensor Networks*. Apr. 2011, pp. 73–84 (cit. on pp. 3, 10, 12, 65, 66, 77, 78, 83, 99).

[27] Cengiz Gezer, Chiara Buratti, and Roberto Verdone. "Capture effect in IEEE 802.15. 4 networks: Modelling and experimentation." In: *Wireless Pervasive Computing (ISWPC), 2010 5th IEEE International Symposium on*. IEEE. 2010, pp. 204–209 (cit. on p. 11).

[28] Francesco Gringoli, Robin Klose, Matthias Hollick, and Nahla Ali. "Making Wi-Fi Fit for the Tactile Internet: Low-Latency Wi-Fi Flooding Using Concurrent Transmissions." In: *2018 IEEE International Conference on Communications Workshops (ICC Workshops)*. IEEE. 2018, pp. 1–6 (cit. on pp. 3, 91).

[29] Zhitao He, Kasun Hewage, and Thiemo Voigt. "Arpeggio: a penetration attack on glossy networks." In: *Sensing, Communication, and Networking (SECON), 2016 13th Annual IEEE International Conference on*. IEEE. 2016, pp. 1–9 (cit. on pp. 12, 99).

[30] Kasun Hewage, Shahid Raza, and Thiemo Voigt. "An experimental study of attacks on the availability of Glossy." In: *Computers & Electrical Engineering* 41 (2015), pp. 115–125 (cit. on pp. 12, 99).

[31] Kasun Chandranath Hewage, Shahid Raza, and Thiemo Voigt. "Protecting Glossy-based Wireless Networks from Packet Injection Attacks." In: *2017 IEEE 14th International Conference on Mobile Ad Hoc and Sensor Systems (MASS)*. IEEE. 2017, pp. 37–45 (cit. on pp. 12, 99).

[32] "IEEE Standard for Information Technology - Telecommunications and Information Exchange Between Systems - Local and Metropolitan Area Networks Specific Requirements Part 15.4: Wireless Medium Access Control (MAC) and Physical Layer (PHY) Specifications for Low-Rate Wireless Personal Area Networks (LR-WPANs)." In: *IEEE Std 802.15.4-2003* (2003). DOI: 10.1109/IEEESTD.2003.94389 (cit. on pp. 66, 68, 69, 72, 78).

[33] Romain Jacob, Jonas Baechli, Reto Da Forno, and Lothar Thiele. "Synchronous Transmissions Made Easy: Design Your Network Stack with Baloo." In: *EWSN* (2019) (cit. on pp. 10, 12).

[34] Furqan Jameel, Shurjeel Wyne, Muhammad Awais Javed, and Sherali Zeadally. "Interference-Aided Vehicular Networks: Future Research Opportunities and Challenges." In: *IEEE Communications Magazine* 56.10 (2018), pp. 36–42 (cit. on p. 14).

[35] Benjamin Kempke, Pat Pannuto, Bradford Campbell, and Prabal Dutta. "SurePoint: Exploiting ultra wideband flooding and diversity to provide robust, scalable, high-fidelity indoor localization." In: *Proceedings of the 14th ACM Confer-*

ence on Embedded Network Sensor Systems CD-ROM. ACM. 2016, pp. 137–149 (cit. on p. 12).

[36] Jirka Klaue, Angel Corona, Martin Kubisch, Javier Garcia-Jimenez, and Antonio Escobar. "Competition: RedFixHop." In: *Proceedings of the 2016 International Conference on Embedded Wireless Systems and Networks*. EWSN '16. Graz, Austria: Junction Publishing, 2016, pp. 289–290. URL: http://dl.acm.org/citation.cfm?id=2893711.2893778 (cit. on pp. 6, 12, 65, 73, 75).

[37] Michael König and Roger Wattenhofer. "Effectively capturing attention using the capture effect." In: *Proceedings of the 14th ACM Conference on Embedded Network Sensor Systems*. ACM. 2016, pp. 70–82 (cit. on p. 59).

[38] Chun-Hao Liao, Yuki Katsumata, Makoto Suzuki, and Hiroyuki Morikawa. "Revisiting the so-called constructive interference in concurrent transmission." In: *Local Computer Networks (LCN), 2016 IEEE 41st Conference on*. IEEE. 2016, pp. 280–288 (cit. on pp. 10, 41, 82, 94).

[39] Chun-Hao Liao, Guibing Zhu, Daiki Kuwabara, Makoto Suzuki, and Hiroyuki Morikawa. "Multi-hop LoRa networks enabled by concurrent transmission." In: *IEEE Access* 5 (2017), pp. 21430–21446 (cit. on p. 12).

[40] Roman Lim, Reto Da Forno, Felix Sutton, and Lothar Thiele. "Competition: Robust flooding using back-to-back synchronous transmissions with channel-hopping." In: *Proceedings of the European Conference on Wireless Sensor Networks (EWSN)*. 2017 (cit. on p. 12).

[41] Fabian Mager, Dominik Baumann, Romain Jacob, Lothar Thiele, Sebastian Trimpe, and Marco Zimmerling. "Feedback Control Goes Wireless: Guaranteed Stability over Low-power Multi-hop Networks." In: *arXiv preprint arXiv:1804.08986* (2018) (cit. on p. 13).

[42] Fabian Mager, Dominik Baumann, Sebastian Trimpe, and Marco Zimmerling. "Toward fast closed-loop control over multi-hop low-power wireless networks." In: *Proceedings of the 17th ACM/IEEE International Conference on Information*

Processing in Sensor Networks. IEEE Press. 2018, pp. 158–159 (cit. on p. 13).

[43] Rainer Matischek, Markus Dielacher, Martin Flatscher, Thomas Herndl, and Josef Prainsack. "Optimized Protocol Processing for a Low-Power Wireless Senor Node." In: *23th International Conference on Architecture of Computing Systems* (2010) (cit. on p. 75).

[44] Claro Noda, Carlos M Pérez-Penichet, Balint Seeber, Marco Zennaro, Mário Alves, and Adriano Moreira. "On the scalability of constructive interference in low-power wireless networks." In: *European Conference on Wireless Sensor Networks*. Springer. 2015, pp. 250–257 (cit. on pp. 10, 95).

[45] James E Palmer, H Andrew Harms, Stephen J Searle, and LindaM Davis. "DVB-T passive radar signal processing." In: *IEEE transactions on Signal Processing* 61.8 (2013), pp. 2116–2126 (cit. on p. 11).

[46] Subbarayan Pasupathy. "Minimum shift keying: A spectrally efficient modulation." In: *IEEE Communications Magazine* 17.4 (1979), pp. 14–22 (cit. on p. 82).

[47] K Pister and Lance Doherty. "TSMP: Time synchronized mesh protocol." In: *IASTED Distributed Sensor Networks* (2008), pp. 391–398 (cit. on pp. 66, 67).

[48] J.G. Proakis and M. Salehi. *Digital Communications*. McGraw-Hill, 2008. URL: `https://books.google.de/books?id=ABSmAQAACAAJ` (cit. on pp. 19, 34, 47).

[49] Philipp Schulz et al. "Latency critical IoT applications in 5G: Perspective on the design of radio interface and network architecture." In: *IEEE Communications Magazine* 55.2 (2017), pp. 70–78 (cit. on p. 13).

[50] Weisong Shi, Jie Cao, Quan Zhang, Youhuizi Li, and Lanyu Xu. "Edge computing: Vision and challenges." In: *IEEE Internet of Things Journal* 3.5 (2016), pp. 637–646 (cit. on p. 9).

[51] Stelios Timotheou, Gan Zheng, Christos Masouros, and Ioannis Krikidis. "Exploiting constructive interference for simultaneous wireless information and power transfer in multiuser downlink systems." In: *IEEE Journal on Selected Areas in Communications* 34.5 (2016), pp. 1772–1784 (cit. on p. 14).

[52] Matthew C Valenti, Don Torrieri, and Terry Ferrett. "Noncoherent physical-layer network coding with FSK modulation: Relay receiver design issues." In: *IEEE Transactions on Communications* 59.9 (2011), pp. 2595–2604 (cit. on p. 45).

[53] Y. Wang, Y. Liu, Y. He, X. Y. Li, and D. Cheng. "Disco: Improving Packet Delivery via Deliberate Synchronized Constructive Interference." In: *IEEE Transactions on Parallel and Distributed Systems* 26.3 (Mar. 2015), pp. 713–723. DOI: 10.1109/TPDS.2014.2312198 (cit. on pp. 65, 78).

[54] Yin Wang, Yuan He, Xufei Mao, Yunhao Liu, and Xiangyang Li. "Exploiting constructive interference for scalable flooding in wireless networks." In: *IEEE/ACM Transactions on Networking* 21.6 (2013), pp. 1880–1889 (cit. on p. 72).

[55] Thomas Watteyne, M Palattella, and L Grieco. *Using IEEE 802.15. 4e Time-Slotted Channel Hopping (TSCH) in the Internet of Things (IoT): Problem Statement*. RFC. RFC Editor, 2015. URL: https://www.rfc-editor.org/rfc/rfc7554.txt (cit. on pp. 66, 69).

[56] K. Whitehouse, A. Woo, F. Jiang, J. Polastre, and D. Culler. "Exploiting the Capture Effect for Collision Detection and Recovery." In: *The Second IEEE Workshop on Embedded Networked Sensors, 2005. EmNetS-II.* May 2005, pp. 45–52. DOI: 10.1109/EMNETS.2005.1469098 (cit. on pp. 68, 78).

[57] Matthias Wilhelm, Vincent Lenders, and Jens B Schmitt. "On the reception of concurrent transmissions in wireless sensor networks." In: *IEEE Transactions on Wireless Communications* 13.12 (2014), pp. 6756–6767 (cit. on pp. 10, 33, 35, 76).

[58] Vincent WS Wong, Robert Schober, Derrick Wing Kwan Ng, and Li-Chun Wang. *Key technologies for 5G wireless systems*. Cambridge university press, 2017 (cit. on p. 4).

[59] O. N. C. Yilmaz, Y. -. E. Wang, N. A. Johansson, N. Brahmi, S. A. Ashraf, and J. Sachs. "Analysis of ultra-reliable and low-latency 5G communication for a factory automation use case." In: *2015 IEEE International Conference on Communication Workshop (ICCW)*. June 2015, pp. 1190–1195. DOI: 10.1109/ICCW.2015.7247339 (cit. on p. 4).

[60] Shuying Yu, Xiaobing Wu, Pan Wu, Dingming Wu, Haipeng Dai, and Guihai Chen. "CIRF: Constructive interference-based reliable flooding in asynchronous duty-cycle wireless sensor networks." In: *WCNC*. 2014, pp. 2734–2738 (cit. on p. 12).

[61] Dingwen Yuan and Matthias Hollick. "Let's talk together: Understanding concurrent transmission in wireless sensor networks." In: *Local Computer Networks (LCN), 2013 IEEE 38th Conference on*. IEEE. 2013, pp. 219–227 (cit. on p. 10).

[62] Dingwen Yuan, Michael Riecker, and Matthias Hollick. "Making 'Glossy' Networks Sparkle: Exploiting Concurrent Transmissions for Energy Efficient, Reliable, Ultra-Low Latency Communication in Wireless Control Networks." In: *Wireless Sensor Networks: 11th European Conference, EWSN 2014, Oxford, UK, February 17-19, 2014, Proceedings*. Ed. by Bhaskar Krishnamachari, Amy L. Murphy, and Niki Trigoni. Cham: Springer International Publishing, 2014, pp. 133–149. DOI: 10.1007/978-3-319-04651-8_9. URL: https://doi.org/10.1007/978-3-319-04651-8_9 (cit. on pp. 65, 78).

[63] Georg von Zengen, Alexander Baumstark, Alexander Willecke, Ulf Kulau, and Lars Wolf. "How Different Transceiver Hardware Effects Concurrent Transmissions in WSNs." In: *2018 14th International Conference on Distributed Computing in Sensor Systems (DCOSS)*. IEEE. 2018, pp. 139–146 (cit. on p. 11).

[64] Georg von Zengen, Alexander Willecke, and Lars C Wolf. "Investigating Concurrent Transmission Using Software Defined Radios." In: *EWSN* (2018) (cit. on p. 11).

[65] Xin Ming Zhang, Long Yan, Hui Zhang, and Dan Keun Sung. "A concurrent transmission based broadcast scheme for urban VANETs." In: *IEEE Transactions on Mobile Computing* 18.1 (2019), pp. 1–12 (cit. on p. 14).

[66] Mohammed Abdullah Zubair, Ajay Kumar Nain, Jagadish Bandaru, Pachamuthu Rajalakshmi, and Uday B Desai. "Reconfigurable dual mode ieee 802.15. 4 digital baseband receiver for diverse iot applications." In: *2016 IEEE 3rd World Forum on Internet of Things (WF-IoT)*. IEEE. 2016, pp. 389–394 (cit. on p. 94).

CURRICULUM VITAE

NAME: Antonio David Escobar Molero

DOB: November 30, 1989

POB: Almería, Spain

NATIONALITY: Spanish

WORK EXPERIENCE

08/2018–PRESENT: Senior R&D Engineer, Infineon Technologies AG

08/2016–07/2018: PhD Student, Infineon Technologies AG

03/2014–07/2016: R&D Engineer, Infineon Technologies AG

07/2013–03/2014: Feb 2014 Internship, Infineon Technologies AG

EDUCATION

2015–2020: PhD Candidate, RWTH Aachen University

2012–2016: M.Sc. Electronic Engineering, University of Granada

2007–2013: M.Sc. Telecommunications Engineering, University of Granada

AWARDS

2019: EWSN Dependability Competition. Category 1: Data Collection for Condition Monitoring. Second Place (RedNodeBus).

2019: EWSN Dependability Competition. Category 2: Dissemination of Actuation Commands. First Place (RedNodeBus).

2018: EWSN Dependability Competition. First Place (BigBangBus).

2017: EWSN Dependability Competition. Second Place (RedFixHop).

2016: IEEE SECON. Best Demo Award (RedFixHop).

2016: EWSN Dependability Competition. First Place (RedFixHop).

PUBLICATIONS

Some ideas and figures have appeared previously in the following publications:

[1] Antonio Escobar, Francisco J. Cruz, Javier Garcia-Jimenez, Jirka Klaue, and Angel Corona. "RedFixHop with channel hopping: Reliable ultra-low-latency network flooding." In: *2016 Conference on Design of Circuits and Integrated Systems (DCIS)*. Nov. 2016, pp. 1–4. DOI: 10.1109/DCIS.2016.7845367. URL: https://ieeexplore.ieee.org/document/7845367/.

[2] Antonio Escobar, Javier Garcia-Jimenez, Francisco J. Cruz, Jirka Klaue, Angel Corona, and Divya Tati. "Competition: RedFixHop with Channel Hopping." In: *Proceedings of the 2017 International Conference on Embedded Wireless Systems and Networks*. EWSN '17. Uppsala, Sweden: Junction Publishing, 2017, pp. 264–265. URL: http://dl.acm.org/citation.cfm?id=3108009.3108073.

[3] Antonio Escobar, Cristian Gonzalez, Francisco J. Cruz, Javier Garcia-Jimenez, Jirka Klaue, and Angel Corona. "RedFixHop: Efficient Ultra-Low-Latency Network Flooding." In: *2016 13th Annual IEEE International Conference on Sensing, Communication, and Networking (SECON)*. June 2016, pp. 1–2. DOI: 10.1109/SAHCN.2016.7733012. URL: https://ieeexplore.ieee.org/document/7733012/.

[4] Antonio Escobar, Fernando Moreno, Antonio J Cabrera, Javier Garcia-Jimenez, Francisco J Cruz, Jirka Klaue, Angel Corona, Divya Tati, and Diego P Morales. "Demo: RedFixHop - Reliable Real-Time Network Flooding." In: *Proceedings of the 2018 International Conference on Embedded Wireless Systems and Networks*. Junction Publishing. 2018, pp. 197–198. URL: http://dl.acm.org/citation.cfm?id=3234885.

[5] Antonio Escobar et al. “Competition: BigBangBus.” In: *Proceedings of the 2018 International Conference on Embedded Wireless Systems and Networks*. Junction Publishing. 2018, pp. 213–214. URL: http://dl.acm.org/citation.cfm?id=3234894.

[6] Antonio Escobar-Molero. “Improving reliability and latency of Wireless Sensor Networks using Concurrent Transmissions.” In: *at - Automatisierungstechnik* 67.1 (Jan. 2019), pp. 42–50. DOI: 10.1515/auto-2018-0064.

[7] Antonio Escobar-Molero, Javier Garcia-Jimenez, Jirka Klaue, Fernando Moreno-Cruz, Borja Saez, Francisco J Cruz, Unai Ruiz, and Angel Corona. “Competition: RedNodeBus, Stretching Out the Preamble.” In: *Proceedings of the 2019 International Conference on Embedded Wireless Systems and Networks*. 2019.

[8] Jirka Klaue, Angel Corona, Martin Kubisch, Javier Garcia-Jimenez, and Antonio Escobar. “Competition: RedFixHop.” In: *Proceedings of the 2016 International Conference on Embedded Wireless Systems and Networks*. EWSN ’16. Graz, Austria: Junction Publishing, 2016, pp. 289–290. URL: http://dl.acm.org/citation.cfm?id=2893711.2893778.

[9] Beshr Al Nahas, Antonio Escobar-Molero, Jirka Klaue, Simon Duquennoy, and Olaf Landsiedel. “BlueFlood: Concurrent Transmissions for Multi-Hop Bluetooth 5–Modeling and Evaluation.” In: *CORR – arXiv preprint 2002.12906* (Feb. 2020).